

## Translocation of copper within the cavity of cryptands: reversible fluorescence signaling

Kalyan Kumar Sadhu and Parimal K. Bharadwaj\*

Department of Chemistry, Indian Institute of Technology Kanpur, 208016, India  
Email: [pkb@iitk.ac.in](mailto:pkb@iitk.ac.in)

### Supporting Information

#### Experimental Section

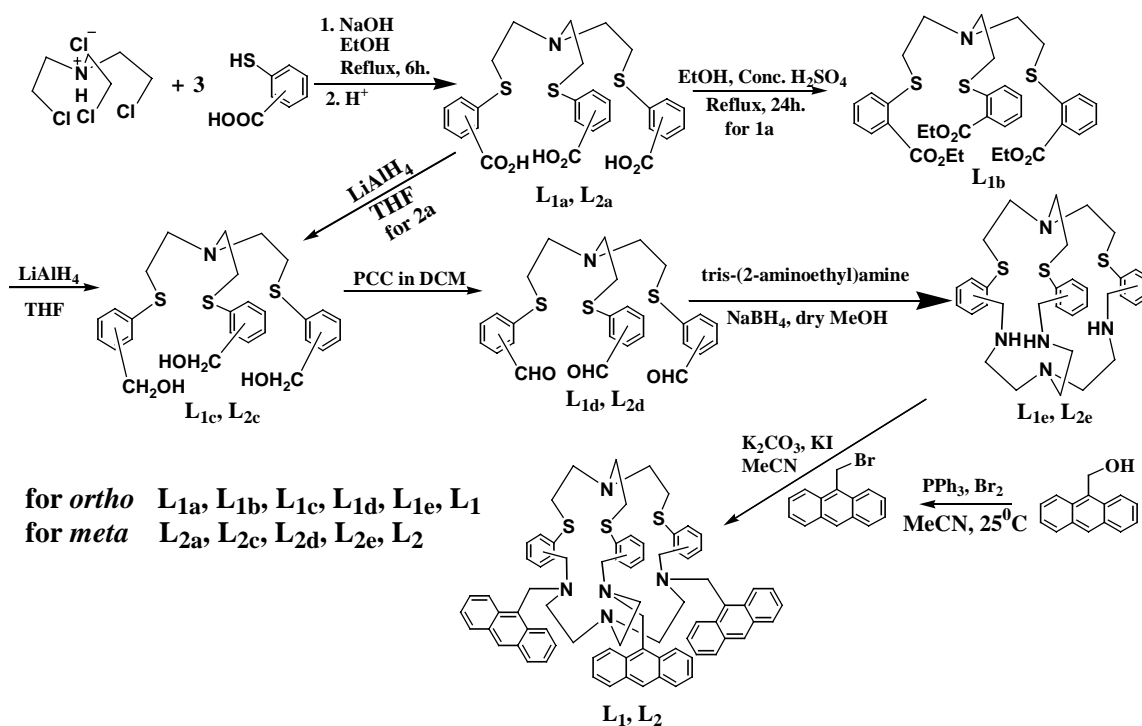
##### Materials.

All solvents and thionyl chloride were purified prior to use. The purified solvents were found to be free from impurities, moisture and were transparent in the region of interest. All other reagent grade chemicals including metal salts were acquired from Aldrich that were used as received. The metal salts were hydrated as mentioned in the Aldrich catalogue. For chromatographic separation, 100-200 mesh silica gel (Acme Synthetic Chemicals) was used. The reactions were carried out under N<sub>2</sub> atmosphere unless otherwise mentioned. Tris(2-chloroethyl)amine hydrochloride was prepared following a literature procedure. 9-Bromomethylanthracene was prepared from 9-hydroxymethylanthracene following a reported method.

##### Physical measurements

The compounds were characterized by elemental analyses, <sup>1</sup>H-NMR, <sup>13</sup>C-NMR and mass (positive ion) spectroscopy. <sup>1</sup>H-NMR and <sup>13</sup>C-NMR spectra were recorded on a JEOL JNM-LA400 FT (400 MHz and 100 MHz respectively) instrument in CDCl<sub>3</sub> or in DMSO-*d*<sup>6</sup> with Me<sub>4</sub>Si as the internal standard. ESI mass spectra were recorded on a WATERS Q-TOF Premier mass spectrometer. The ESI capillary was set at 2.8 kV and the cone voltage was 30V. FAB mass (positive ion) data were obtained from a JEOL SX 102 /DA-6000 mass spectrometer using argon as the FAB gas at 6 kV and 10 mA with an accelerating voltage of 10 kV and the spectra were recorded at 298 K. Melting points were determined with an electrical melting point apparatus by PERFIT, India and were uncorrected. UV-visible spectra were recorded on a JASCO V-570 spectrophotometer in THF solvent at 298 K. Fluorescence spectra were obtained with a Perkin-Elmer LS 50B luminescence spectrometer at 298 K. Fluorescence quantum yields of all the compounds were determined by comparing each spectrum with that of anthracene ( $\phi = 0.297$ ) in ethanol<sup>14</sup> taking the area under the total emission as reference at  $\lambda_{\text{ex}}$  of 350 nm. The error in  $\phi_F$  is 15 % for the free ligand, otherwise 10 % in each case. The fluorescence measurements in solutions were carried out at  $\sim 10^{-6}$  M concentration unless otherwise specified. The complex stability constant  $K_s$  were determined<sup>15</sup> from the change in absorbance or fluorescence intensity resulting from the titration of dilute solutions ( $\sim 10^{-5}$ – $10^{-6}$  M) of the fluorophoric systems against metal ion concentration. The reported values gave good correlation coefficients ( $\geq 0.98$ ). Cyclic voltammetric studies of complexes (conc. ca.  $1 \times 10^{-3}$  M) were performed on a BAS Epsilon electrochemical workstation in THF with 0.1 M tetra-*n*-

butylammonium hexafluorophosphate (TBAPF<sub>6</sub>) as the supporting electrolyte. The working electrode was a BAS glassy carbon electrode; the reference electrode was Ag/AgCl, and the auxiliary electrode was a Pt wire. The scan rate was 100 mV s<sup>-1</sup>. All potentials were referenced to the Ag/AgCl electrode, and under our experimental conditions,  $E_{1/2}$  for the Fc/Fc<sup>+</sup> couple occurred at +0.60 V.



**Scheme:** Synthetic route to the investigated compounds L<sub>1</sub> and L<sub>2</sub>.

**Synthesis of tris{[2-(2-carboxyphenyl)thio]ethyl}amine (L<sub>1a</sub>) and tris{[2-(3-carboxyphenyl)thio]ethyl}amine (L<sub>2a</sub>).** To a solution of 2-/3-mercapto benzoic acid (2.0 g, 13 mmol) in 30 mL dry ethanol taken in a 250 mL round-bottom flask, crushed NaOH (1.4 g, 35 mmol) was added. After stirring for 1 h at 25 °C, tris-(2-chloroethyl)amine hydrochloride (1 g, 4 mmol) was added and the mixture shaken for 30 min. It was then heated under reflux for 6 h. The product after cooling to RT, was acidified with 6 N HCl to obtain a pale yellow solid precipitate for the *ortho* and a brown solid for the *meta* acid. The compounds were collected by filtration, washed several times with water to get desired products.

Compound L<sub>1a</sub> Yield: 93(%); <sup>1</sup>H NMR (400 MHz, DMSO-d<sub>6</sub>, 25 °C, TMS δ): 2.88–2.98 (m, 12H, 6 × CH<sub>2</sub>), 6.74 (d, 3H, Ar-H), 7.58 (m, 3H, Ar-H), 8.16 (d, 3H, Ar-H), 8.73 ppm (m, 3H, Ar-H); mp 170 °C; ESI-MS (m/z): 557 (100%) [L<sub>1a</sub>]<sup>+</sup>. Anal. Calcd. for C<sub>27</sub>H<sub>27</sub>NO<sub>6</sub>S<sub>3</sub>: C, 58.15; H, 4.88; N, 2.51 %. Found: C, 58.18; H, 4.78; N, 2.48 %.

Compound L<sub>2a</sub> Yield: 63(%); <sup>1</sup>H NMR (400 MHz, DMSO-d<sub>6</sub>, 25 °C, TMS δ): 2.78–3.08 (m, 12H, 6 × CH<sub>2</sub>), 6.32 (d, 3H, Ar-H), 7.60 (d, 3H, Ar-H), 8.17 (d, 3H, Ar-H), 8.75 ppm (s, 3H, Ar-H); ESI-MS (m/z): 557 (85%) [L<sub>2a</sub>]<sup>+</sup>. Anal. Calcd. for C<sub>27</sub>H<sub>27</sub>NO<sub>6</sub>S<sub>3</sub>: C, 58.15; H, 4.88; N, 2.51 %. Found: C, 58.13; H, 4.89; N, 2.55 %.

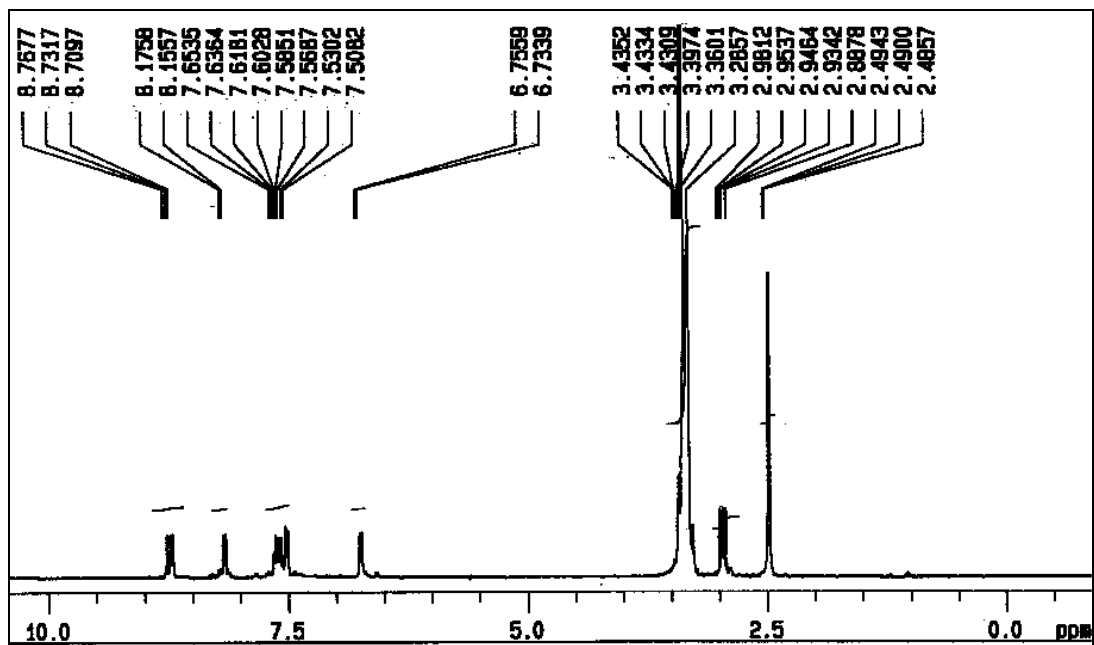


Fig. S1: 400 MHz  $^1\text{H-NMR}$  spectrum of  $\text{L}_{1a}$ .

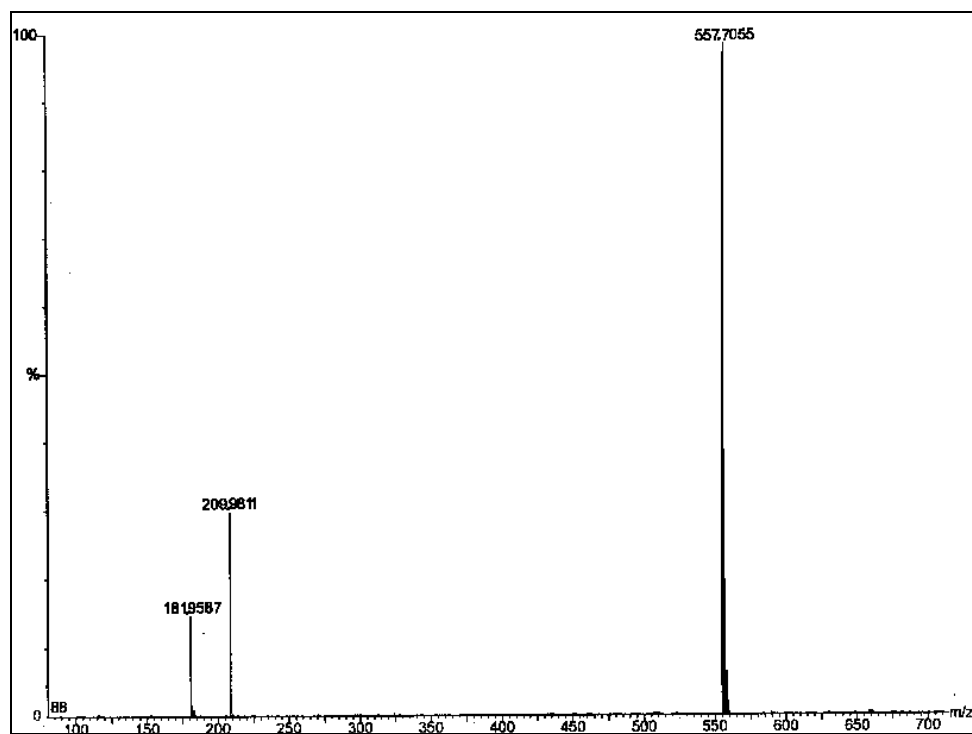


Fig. S2: ESI-MS spectrum of  $\text{L}_{1a}$ .

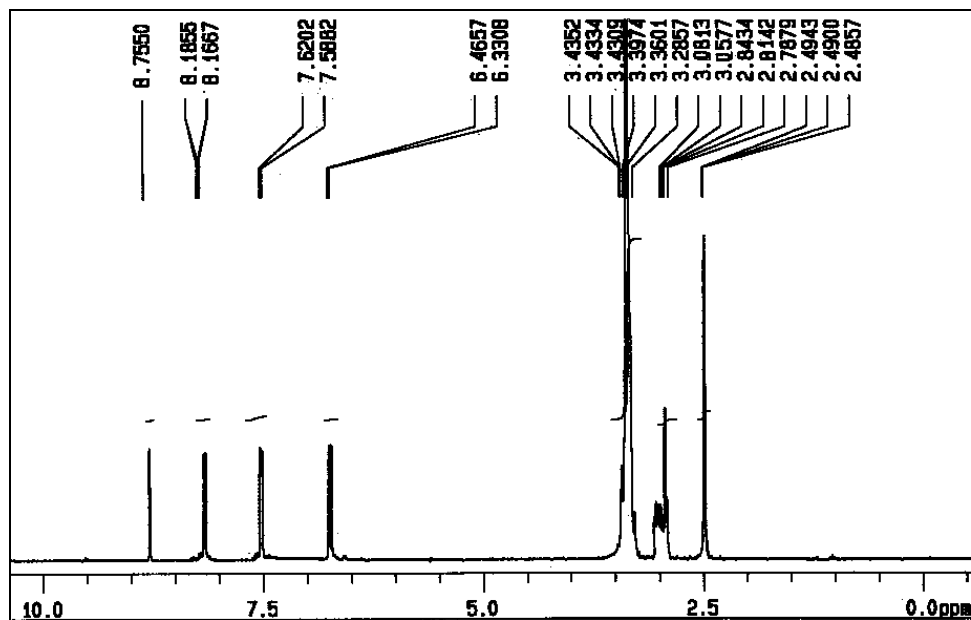


Fig. S3: 400 MHz  $^1\text{H}$ -NMR spectrum of  $\text{L}_{2a}$ .

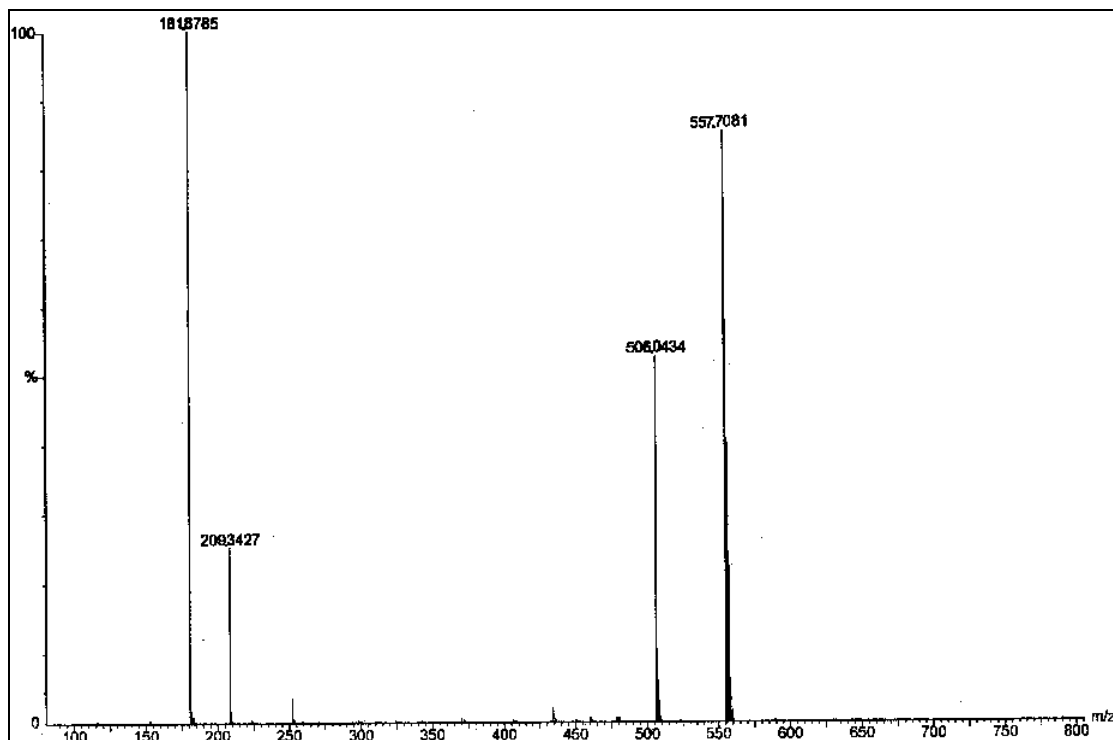


Fig. S4: ESI-MS spectrum of  $\text{L}_{2a}$ .

**Synthesis of tris[2-(2-ethylbenzoate)thio]ethylamine ( $L_{1b}$ ):** The tripodal *ortho* acid obtained in the previous step was then subjected to esterification by reaction with 150 mL dry ethanol and 1 mL conc.  $H_2SO_4$ . It was refluxed for 24 h. The product obtained was extracted with diethyl ether from aqueous solution. The ether layer after drying over anhydrous  $Na_2SO_4$ , was evaporated to obtain the brown semi-solid under vacuum.

Compound  $L_{1b}$  Yield: 68(%);  $^1H$  NMR (400 MHz,  $CDCl_3$ , 25 °C, TMS  $\delta$ ): 1.29 (t, 9H, 3  $\times$   $CH_3$ ), 2.81 (t, 6H, 3  $\times$   $CH_2$ ), 2.95 (t, 6H, 3  $\times$   $CH_2$ ), 4.27 (q, 6H, 3  $\times$   $OCH_2$ ), 7.05 (m, 3H, Ar-H), 7.23 (d, 3H, Ar-H), 7.31 (m, 3H, Ar-H), 7.86 ppm (d of d, 3H, Ar-H);  $^{13}C\{^1H\}$  NMR (100 MHz,  $CDCl_3$ , 25 °C, TMS  $\delta$ ): 166.33, 140.74, 132.15, 131.13, 128.18, 125.56, 123.88, 61.03, 52.34, 29.54, 14.19 ppm; ESI-MS (m/z): 642(100%) [ $L_{1b}+1$ ] $^+$ . Anal. Calcd. for  $C_{33}H_{39}NO_6S_3$ : C, 61.75; H, 6.12; N, 2.18 %. Found: C, 61.78; H, 6.18; N, 2.20 %.

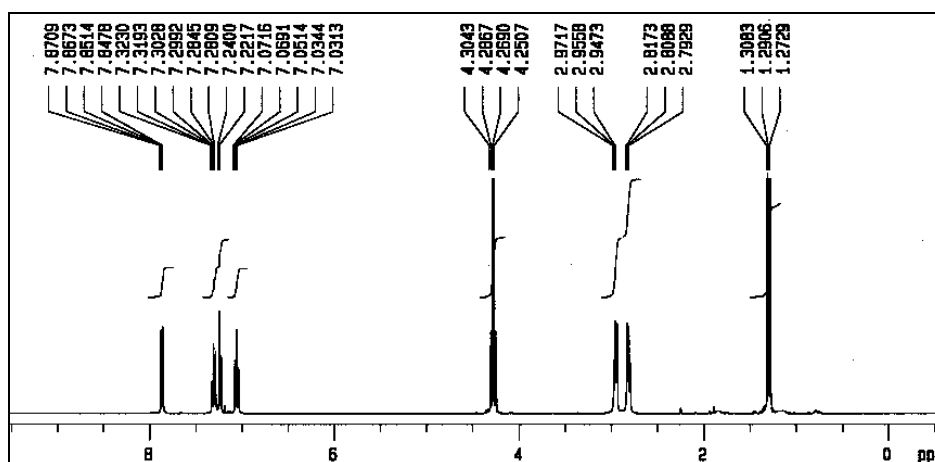


Fig. S5: 400 MHz  $^1H$ -NMR spectrum of  $L_{1b}$ .

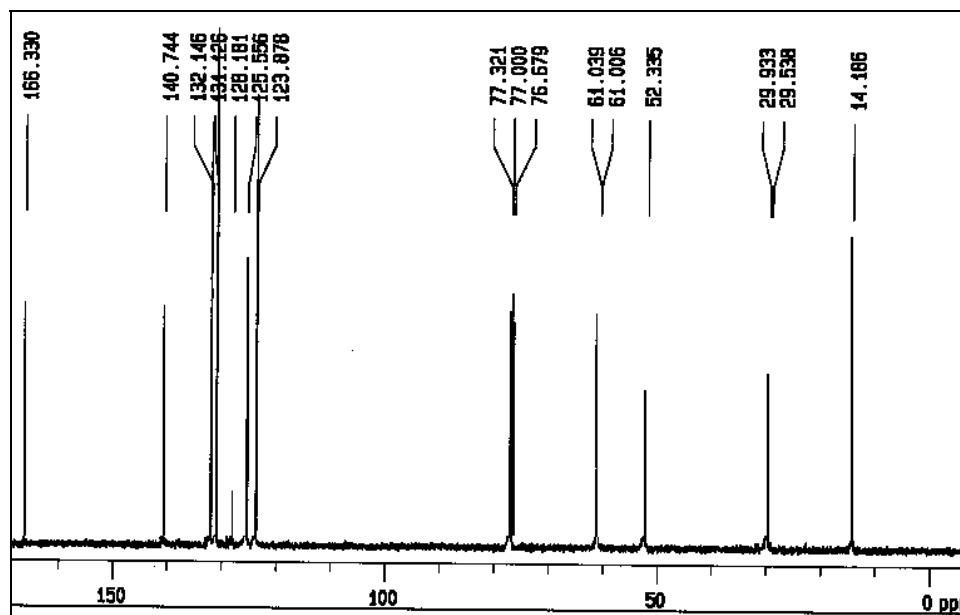


Fig. S6: 100 MHz  $^{13}C$ -NMR spectrum of  $L_{1b}$ .

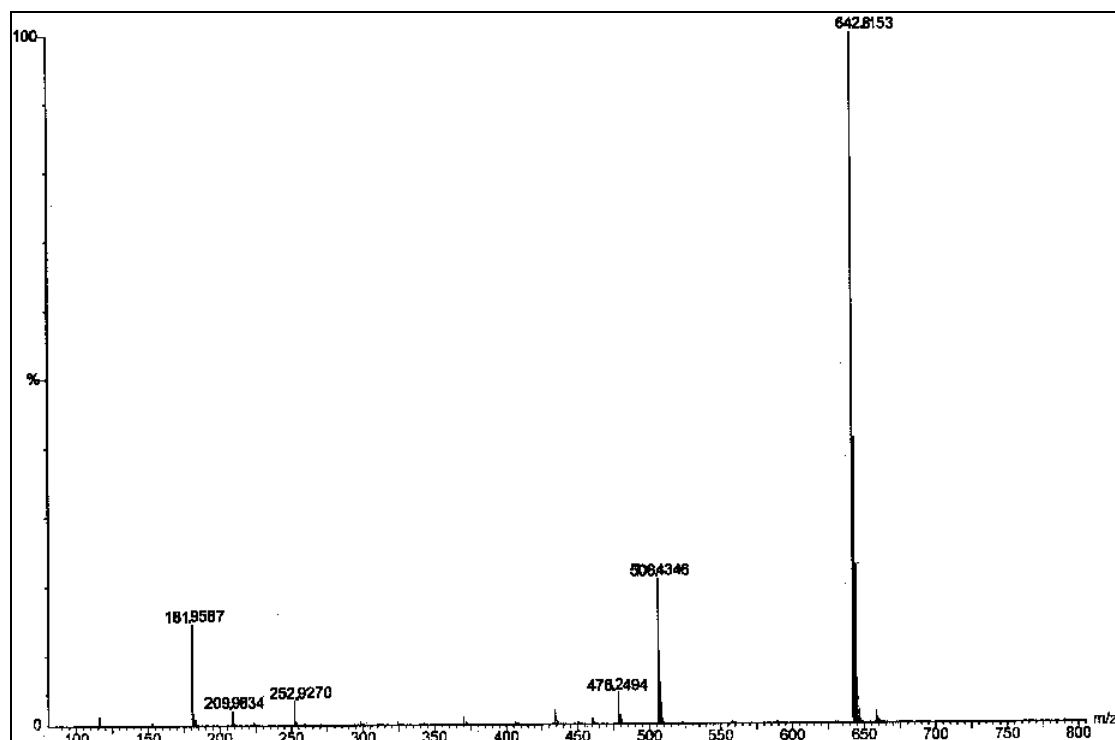


Fig. S7: ESI-MS spectrum of L<sub>1b</sub>.

**Synthesis of Tris[[2-(2-hydroxymethylphenyl)thio]ethyl]amine (L<sub>1c</sub>) and Tris[[2-(3-hydroxymethylphenyl)thio]ethyl]amine (L<sub>2c</sub>).** Reduction of the tripodal ortho ester/tripodal *meta* acid was performed in presence of LiAlH<sub>4</sub> in dry THF. Slight excess of LiAlH<sub>4</sub> (0.2g) was placed inside a 3 necked round-bottom flask containing 50 mL dry THF; it was stirred for 10 min. The ester or acid solution in dry THF was dropwise added to this solution with constant stirring in an ice-bath. After the addition was complete the ice-bath was removed, and it was allowed to stir at room temperature for 24 h. The reaction mixture was quenched with 15 mL ethyl acetate and 10 mL 10% H<sub>2</sub>SO<sub>4</sub>. It was filtered through suction. The filtrate was extracted with ethyl acetate (2 × 20 mL). The organic layer was dried over anhydrous Na<sub>2</sub>SO<sub>4</sub> evaporated and consequently vacuum dried to obtain the alcohols.

Compound L<sub>1c</sub> Yield: 63(%); <sup>1</sup>H NMR (400 MHz, CDCl<sub>3</sub>, 25 °C, TMS δ): 2.52 (t, 6H, 3 × CH<sub>2</sub>), 2.74 (t, 6H, 3 × CH<sub>2</sub>), 4.63 (d, 6H, 3 × OCH<sub>2</sub>), 7.11-7.29 ppm (m, 12H, 3 × 4Ar-H); <sup>13</sup>C{<sup>1</sup>H} NMR (100 MHz, CDCl<sub>3</sub>, 25 °C, TMS δ): 142.06, 133.63, 130.47, 129.57, 128.59, 127.14, 64.86, 63.16, 31.18, 29.59 ppm; ESI-MS (m/z): 518(100%) [L<sub>1c</sub> + 2]<sup>+</sup>. Anal. Calcd. for C<sub>27</sub>H<sub>33</sub>NO<sub>3</sub>S<sub>3</sub>: C, 62.88; H, 6.45; N, 2.72 %. Found: C, 62.78; H, 6.48; N, 2.72 %.

Compound L<sub>2c</sub> Yield: 75(%); <sup>1</sup>H NMR (400 MHz, CDCl<sub>3</sub>, 25 °C, TMS δ): 1.70–2.28 (m, 12H, 6 × CH<sub>2</sub>), 4.62 (s, 6H, 3 × CH<sub>2</sub>), 7.17 (m, 3H, Ar-H), 7.45 (m, 3H, Ar-H), 7.60 (m, 3H, Ar-H), 7.94 ppm (m, 3H, Ar-H); <sup>13</sup>C{<sup>1</sup>H} NMR (100 MHz, CDCl<sub>3</sub>, 25 °C, TMS δ): 151.66, 132.29, 130.62, 129.70, 127.21, 126.05, 64.85, 63.46, 62.47, 32.74, 30.59 ppm; ESI-MS (m/z): 518(75%) [L<sub>2c</sub> + 2]<sup>+</sup>. Anal. Calcd. for C<sub>27</sub>H<sub>33</sub>NO<sub>3</sub>S<sub>3</sub>: C, 62.88; H, 6.45; N, 2.72 %. Found: C, 62.84; H, 6.41; N, 2.73 %.

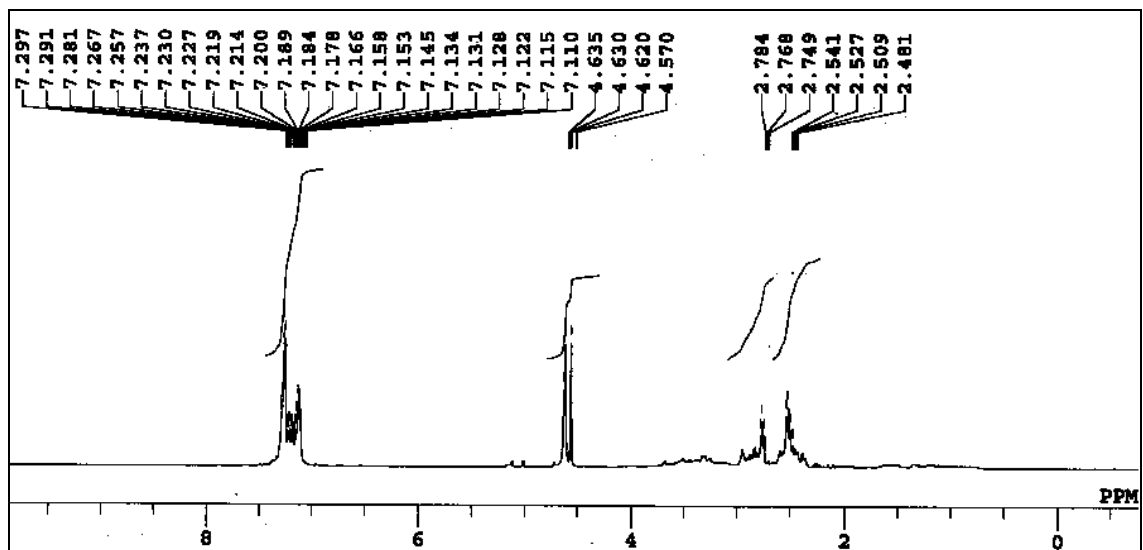


Fig. S8: 400 MHz <sup>1</sup>H-NMR spectrum of L<sub>1c</sub>.

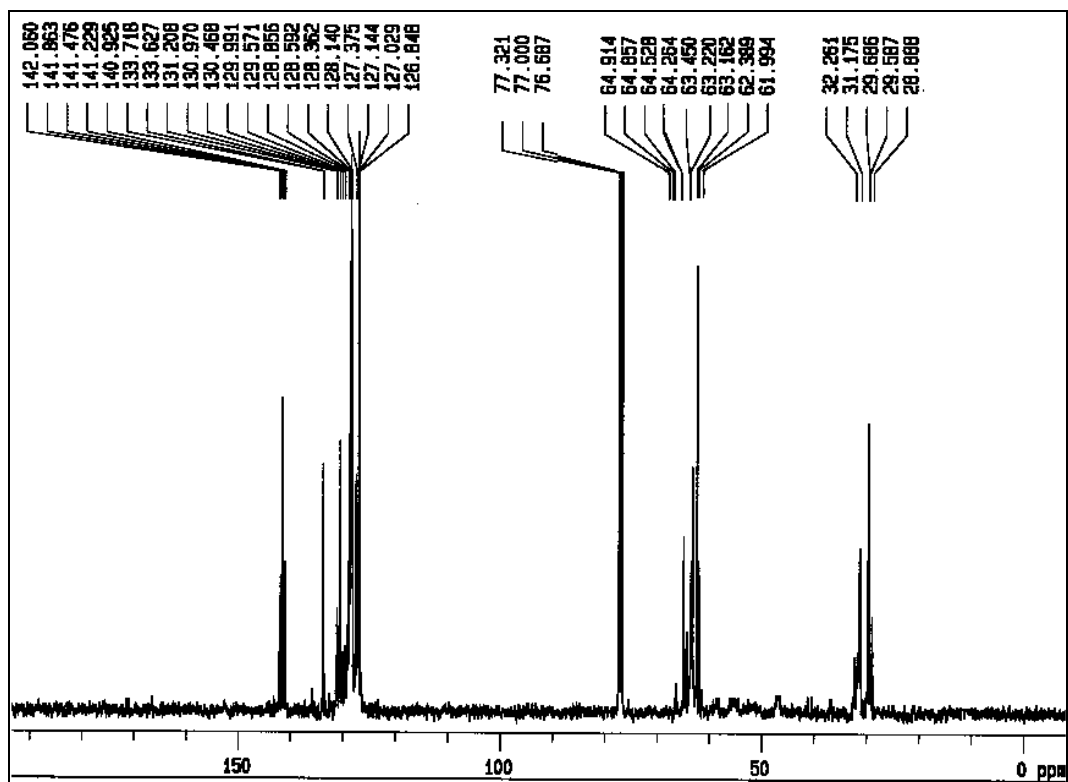


Fig. S9: 100 MHz <sup>13</sup>C-NMR spectrum of L<sub>1c</sub>.

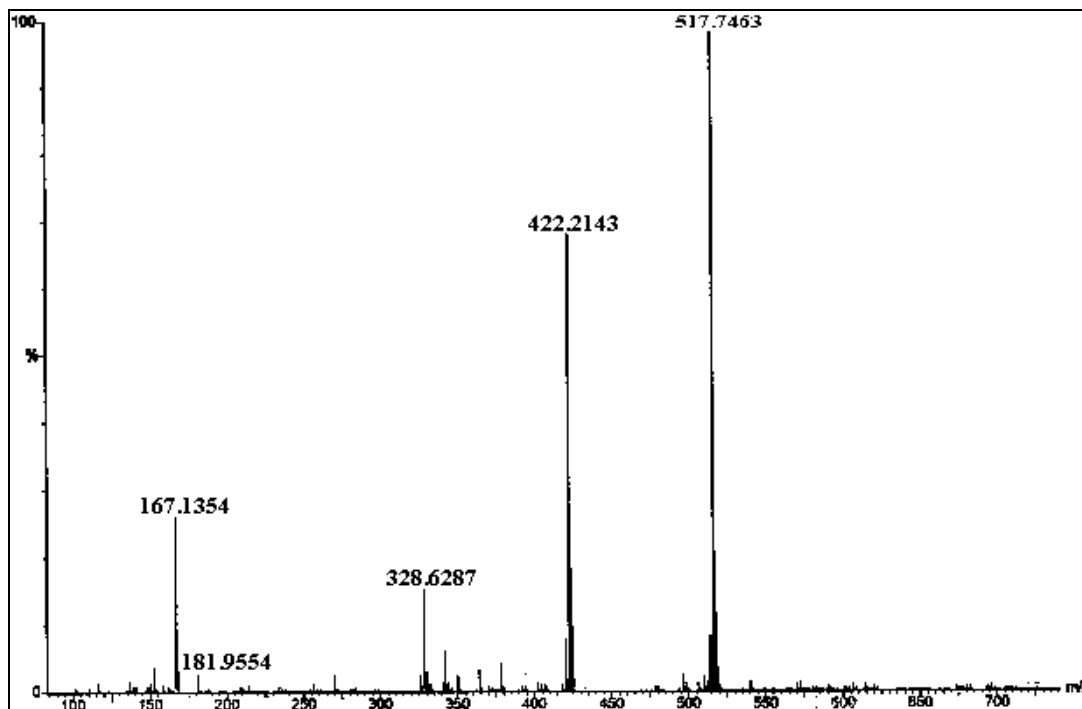


Fig. S10: ESI-MS spectrum of  $L_{1c}$ .

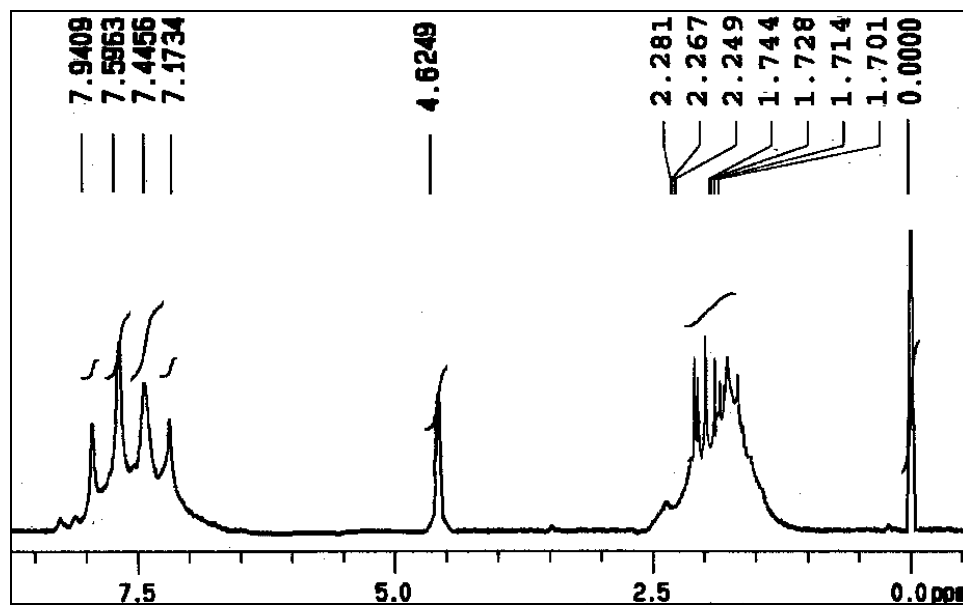


Fig. S11: 400 MHz  $^1H$ -NMR spectrum of  $L_{2c}$ .

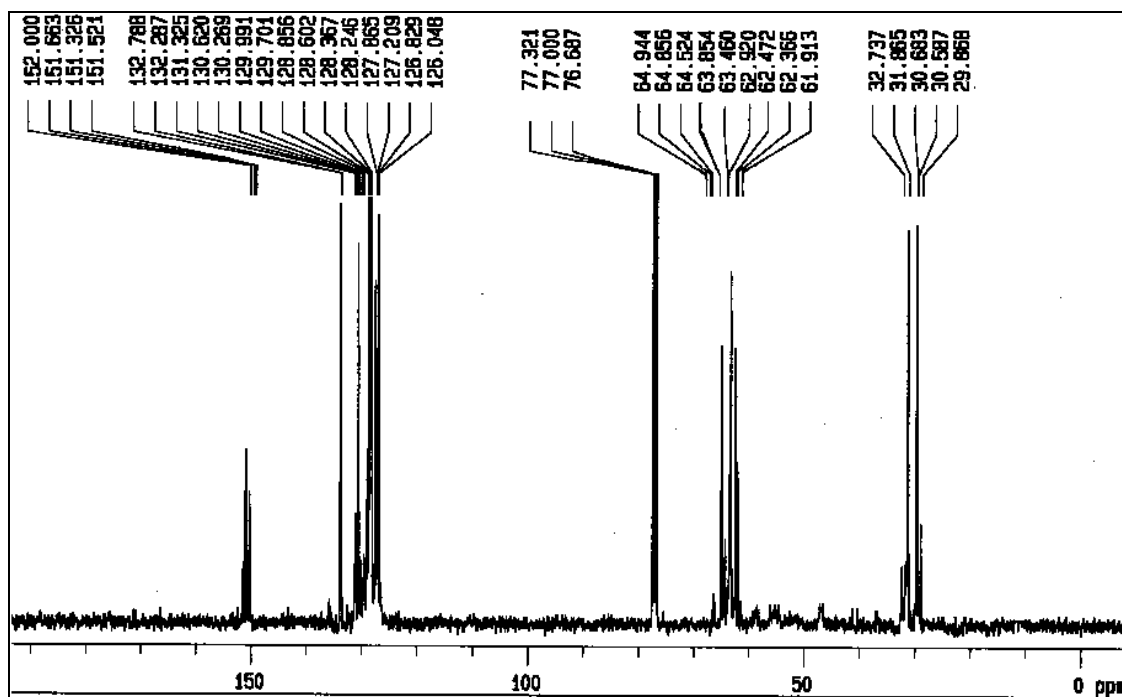


Fig. S12: 100 MHz  $^{13}\text{C}$ -NMR spectrum of  $\text{L}_{2c}$ .

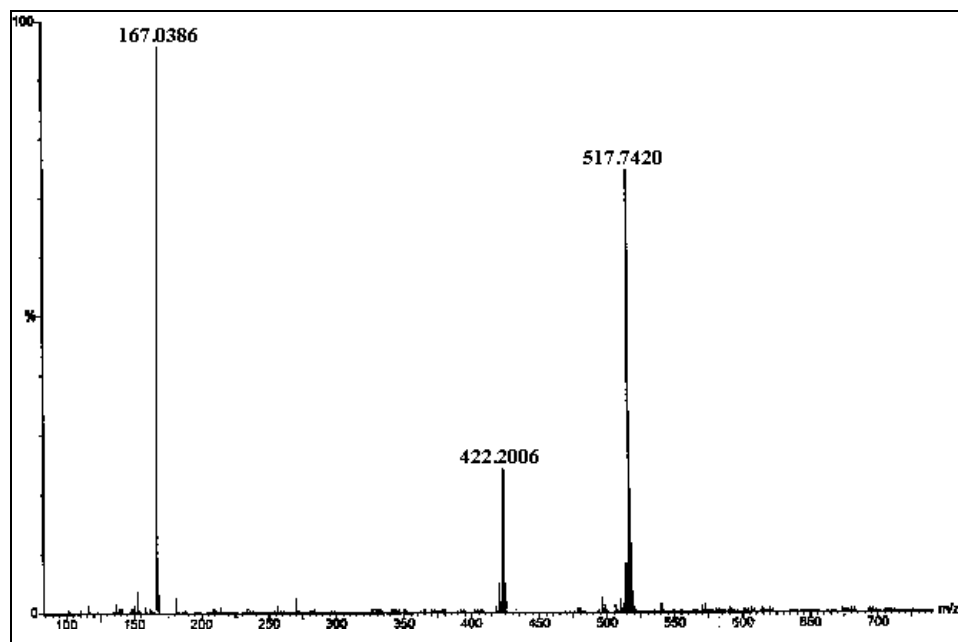
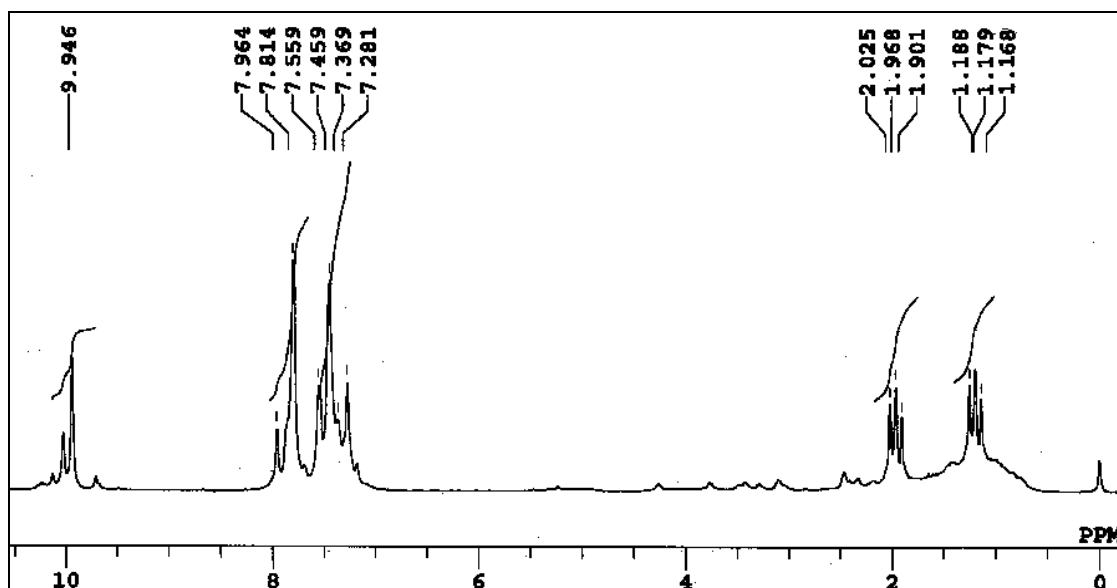


Fig. S13: ESI-MS spectrum of  $\text{L}_{2c}$ .

**Synthesis of Tris[[2-(2-formylphenyl)thio]ethyl]amine (**L<sub>1d</sub>**) and Tris[[2-(3-formylphenyl)thio]ethyl]amine (**L<sub>2d</sub>**):** Each alcohol (0.9 g, 1.7 mmol of **1c** and **2c**) was dissolved separately in 100 mL dry dichloromethane. To each of these PCC (1.1 g, 5.1 mmol) was added. It was stirred for 24 h. Then the solution was filtered through a short pad silica column, it was washed several times with dry dichloromethane. It was washed with water for several times. The organic layer was evaporated after drying over anhydrous Na<sub>2</sub>SO<sub>4</sub> to obtain **L<sub>1d</sub>** and **L<sub>2d</sub>**.

Compound **L<sub>1d</sub>** Yield: 81(%); <sup>1</sup>H NMR (400 MHz, CDCl<sub>3</sub>, 25 °C, TMS δ): 1.17 (t, 6H, 3 × CH<sub>2</sub>), 1.96 (t, 6H, 3 × CH<sub>2</sub>), 7.28 (s, 3H, Ar-H), 7.45 (d, 3H, Ar-H), 7.81 (d, 3H, Ar-H), 7.96 (s, 3H, Ar-H), 9.95 ppm (s, 3H, CHO); <sup>13</sup>C{<sup>1</sup>H} NMR (100 MHz, CDCl<sub>3</sub>, 25 °C, TMS δ): 166.33, 138.74, 132.10, 131.15, 127.19, 125.34, 121.58, 61.03, 52.34 ppm; ESI-MS (m/z): 510 (30%) [**L<sub>1d</sub>**]<sup>+</sup>. Anal. Calcd. for C<sub>27</sub>H<sub>27</sub>NO<sub>3</sub>S<sub>3</sub>: C, 63.62; H, 5.34; N, 2.75 %. Found: C, 63.70; H, 5.38; N, 2.72 %.

Compound **L<sub>2d</sub>** Yield: 83(%); <sup>1</sup>H NMR (400 MHz, CDCl<sub>3</sub>, 25 °C, TMS δ): 1.63 (t, 6H, 3 × CH<sub>2</sub>), 2.01 (t, 6H, 3 × CH<sub>2</sub>), 7.19 (s, 3H, Ar-H), 7.43 (d, 3H, Ar-H), 7.67 (d, 3H, Ar-H), 7.94 (s, 3H, Ar-H), 9.90 ppm (s, 3H, CHO); <sup>13</sup>C{<sup>1</sup>H} NMR (100 MHz, CDCl<sub>3</sub>, 25 °C, TMS δ): 168.37, 140.14, 132.71, 131.12, 128.39, 125.34, 123.58, 62.34, 53.36 ppm; ESI-MS (m/z): 512 (60%) [**L<sub>2d</sub>** + 2]<sup>+</sup>. Anal. Calcd. for C<sub>27</sub>H<sub>27</sub>NO<sub>3</sub>S<sub>3</sub>: C, 63.62; H, 5.34; N, 2.75 %. Found: C, 63.66; H, 5.27; N, 2.80 %.



**Fig. S14:** 400 MHz <sup>1</sup>H-NMR spectrum of **L<sub>1d</sub>**.

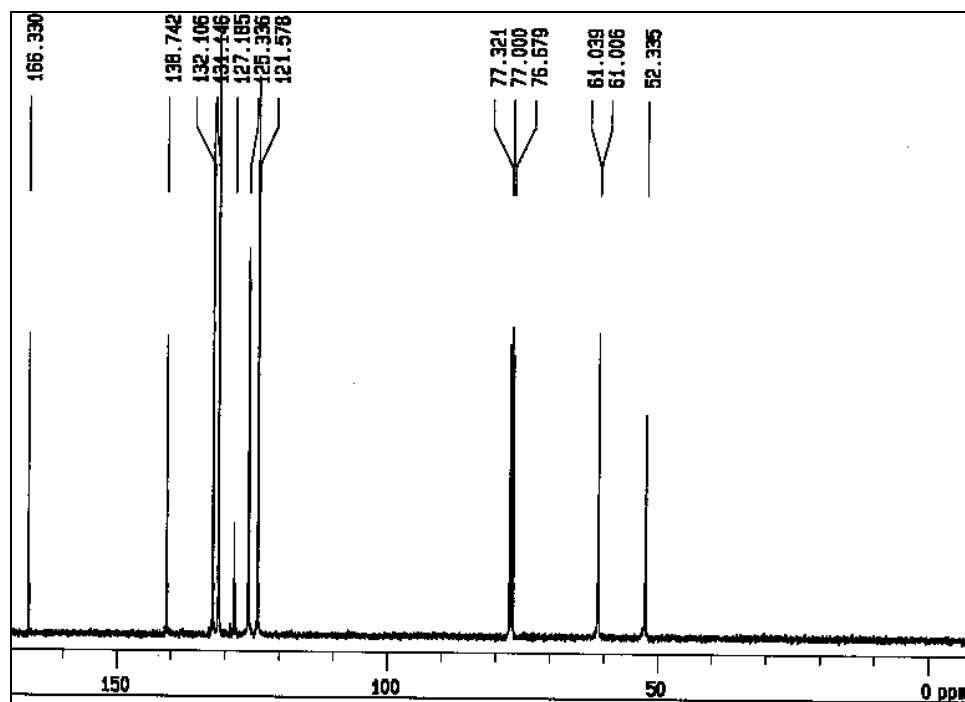


Fig. S15: 100 MHz  $^{13}\text{C}$ -NMR spectrum of  $\text{L}_{1d}$ .

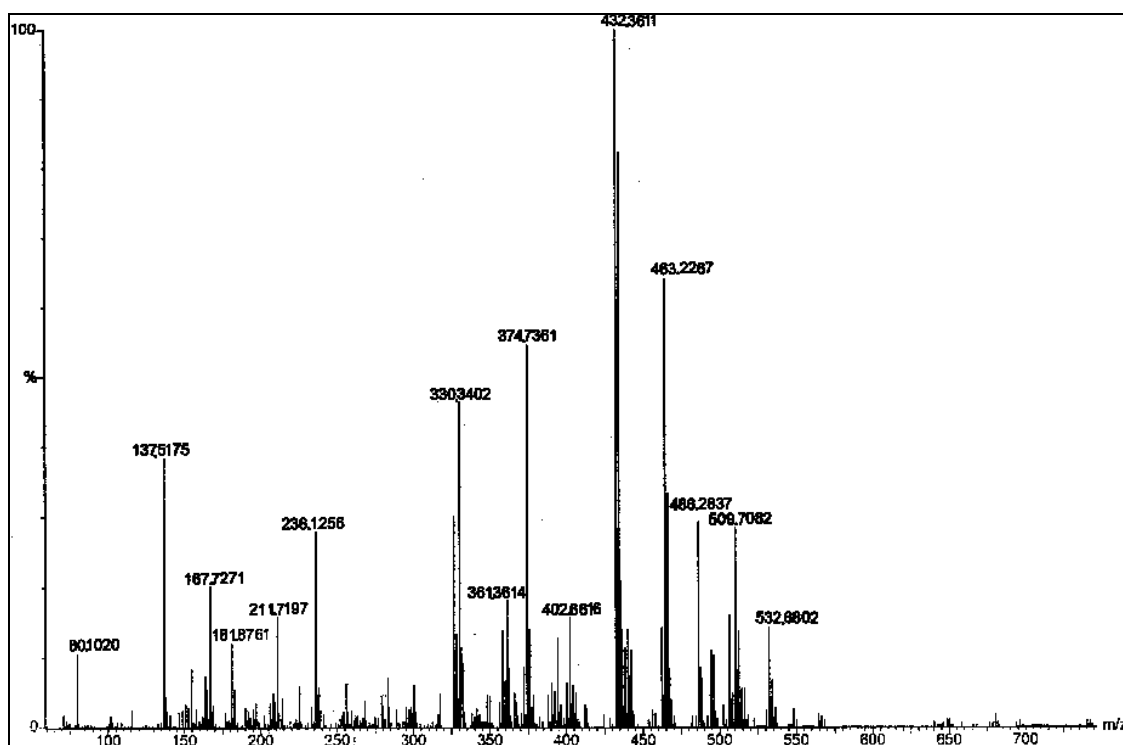


Fig. S16: ESI-MS spectrum of  $\text{L}_{1d}$ .

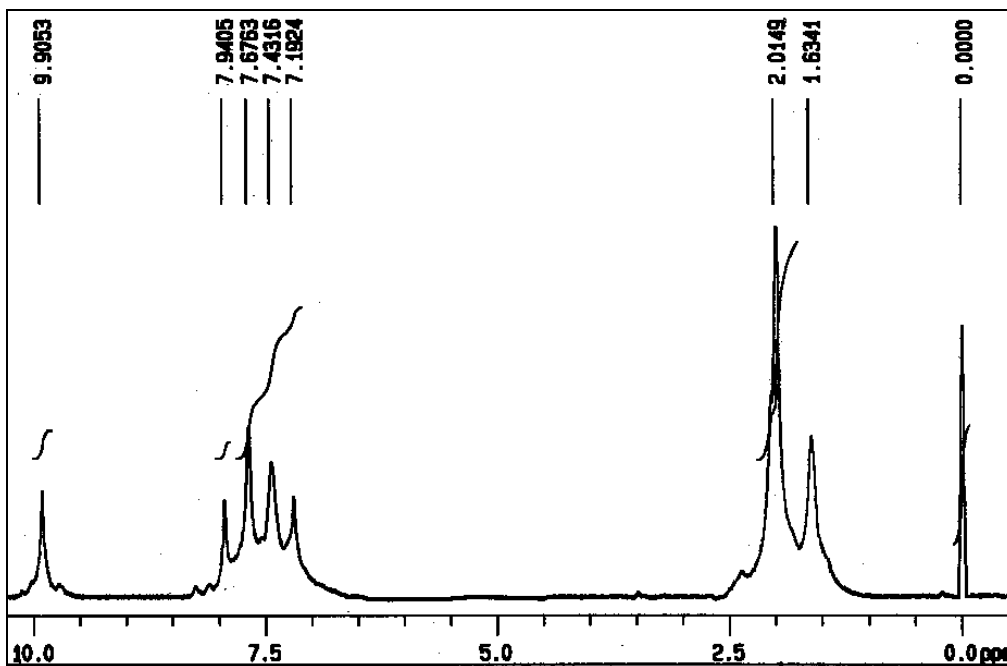


Fig. S17: 400 MHz <sup>1</sup>H-NMR spectrum of L<sub>2d</sub>.

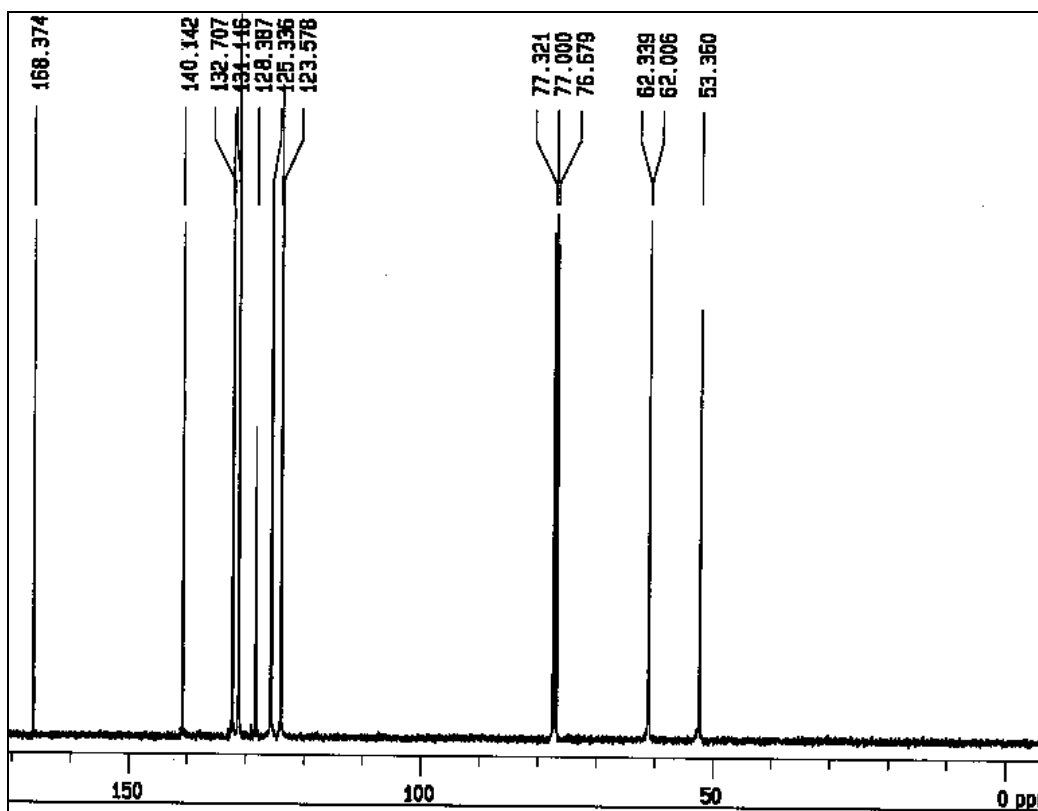


Fig. S18: 100 MHz <sup>13</sup>C-NMR spectrum of L<sub>2d</sub>.

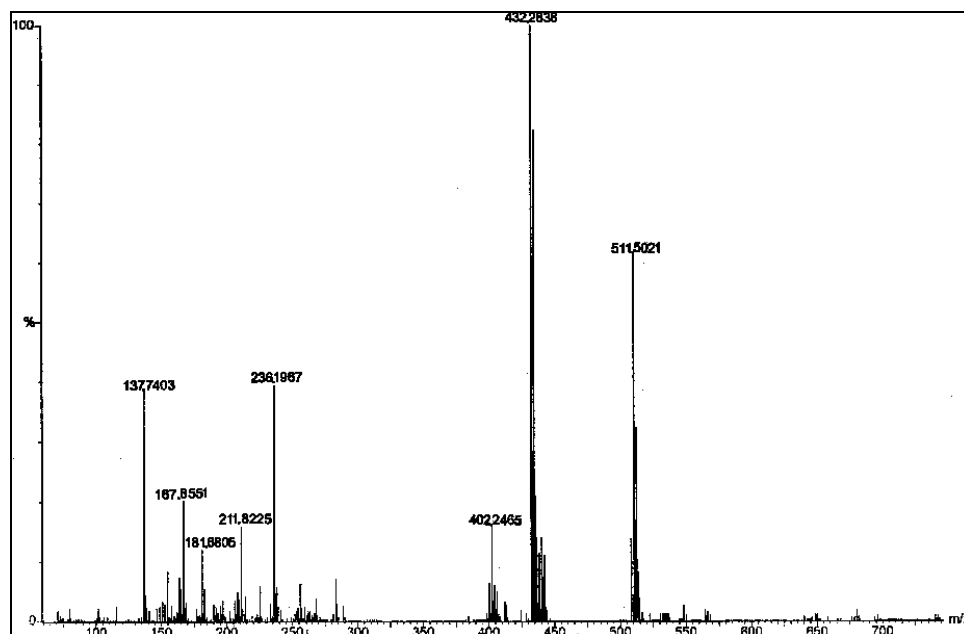


Fig. S19: ESI-MS spectrum of L<sub>2d</sub>.

**Synthesis of Cryptands (L<sub>1e</sub>, L<sub>2e</sub>):** The trialdehyde, L<sub>1d</sub> and L<sub>2d</sub> (0.7 g, 1.4 mmol) were dissolved separately in dry MeOH (100 mL). To each of these, solution of tris-(2-aminoethyl)amine (0.2 mL, 1.4 mmol) taken in dry MeOH (100 mL) was added drop wise over a period of 8 h with constant stirring. After the addition was complete, the light yellow solution was allowed to stir for another 4 h. The Schiff base thus formed was not isolated but treated with excess of solid NaBH<sub>4</sub> (2 g, excess) and stirred for 24 h. Upon evaporating the solvent, the resulting solid was washed with water and the desired cryptand extracted with CHCl<sub>3</sub> (3 × 15 mL). The organic layers after drying over anhydrous Na<sub>2</sub>SO<sub>4</sub> was evaporated to obtain L<sub>1e</sub> and L<sub>2e</sub> as white solids.

Compound L<sub>1e</sub> Yield: 61(%); <sup>1</sup>H NMR (400 MHz, CDCl<sub>3</sub>, 25 °C, TMS δ): 2.74-3.16 (m, 24H, 12 × CH<sub>2</sub>), 3.83 (d, 6H, 3 × CH<sub>2</sub>), 4.29 (t, 3H, NH), 7.03 (m, 3H, Ar-H), 7.22 (m, 3H, Ar-H), 7.35 (m, 3H, Ar-H), 7.86 ppm (m, 3H, Ar-H); <sup>13</sup>C{<sup>1</sup>H} NMR (100 MHz, CDCl<sub>3</sub>, 25 °C, TMS δ): 140.14, 132.25, 131.44, 128.88, 125.79, 123.58, 67.30, 61.04, 57.91 ppm; FAB-MS (m/z): 608 (60%) [L<sub>1e</sub>]<sup>+</sup>. Anal. Calcd. for C<sub>33</sub>H<sub>45</sub>N<sub>5</sub>S<sub>3</sub>: C, 65.20; H, 7.46; N, 11.52 %. Found: C, 65.28; H, 7.48; N, 11.44 %.

Compound L<sub>2e</sub> Yield: 60(%). <sup>1</sup>H NMR (400 MHz, CDCl<sub>3</sub>, 25 °C, TMS δ): 3.24-3.28 (m, 24H, 12 × CH<sub>2</sub>), 5.27 (s, 6H, 3 × CH<sub>2</sub>), 7.21 (m, 3H, Ar-H), 7.34 (m, 3H, Ar-H), 7.39 (m, 3H, Ar-H), 7.52 ppm (m, 3H, Ar-H); <sup>13</sup>C{<sup>1</sup>H} NMR (100 MHz, CDCl<sub>3</sub>, 25 °C, TMS δ): 139.78, 132.25, 131.63, 129.89, 125.56, 123.53, 68.38, 61.34, 58.91 ppm; ESI-MS (m/z): 611 (100%) [L<sub>2e</sub>+3]<sup>+</sup>. Anal. Calcd. for C<sub>33</sub>H<sub>45</sub>N<sub>5</sub>S<sub>3</sub>: C, 65.20; H, 7.46; N, 11.52 %. Found: C, 65.18; H, 7.49; N, 11.50 %.

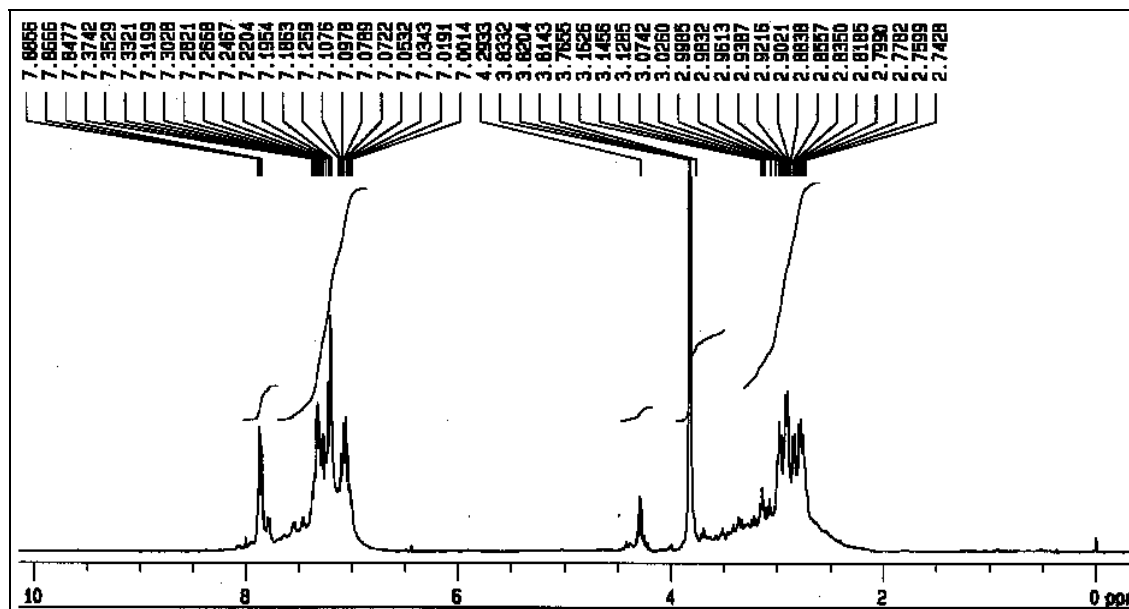


Fig. S20: 400 MHz  $^1\text{H}$ -NMR spectrum of  $\text{L}_{1e}$ .

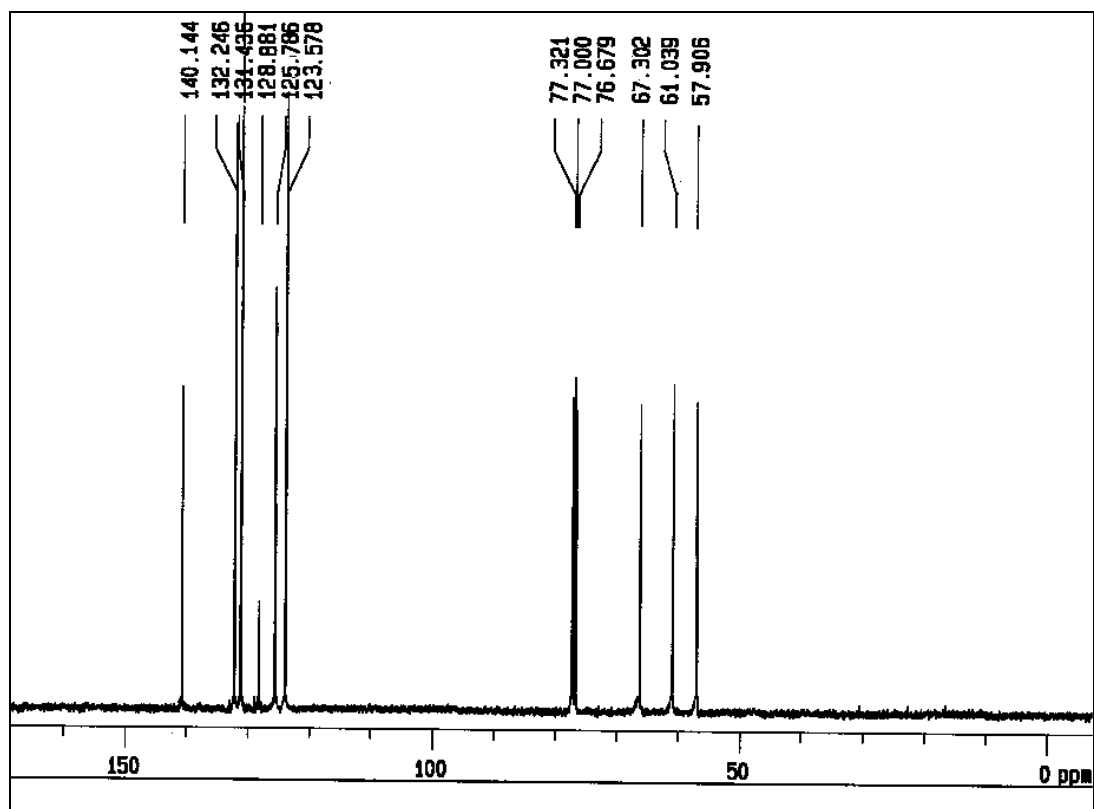


Fig. S21: 100 MHz  $^{13}\text{C}$ -NMR spectrum of  $\text{L}_{1e}$ .

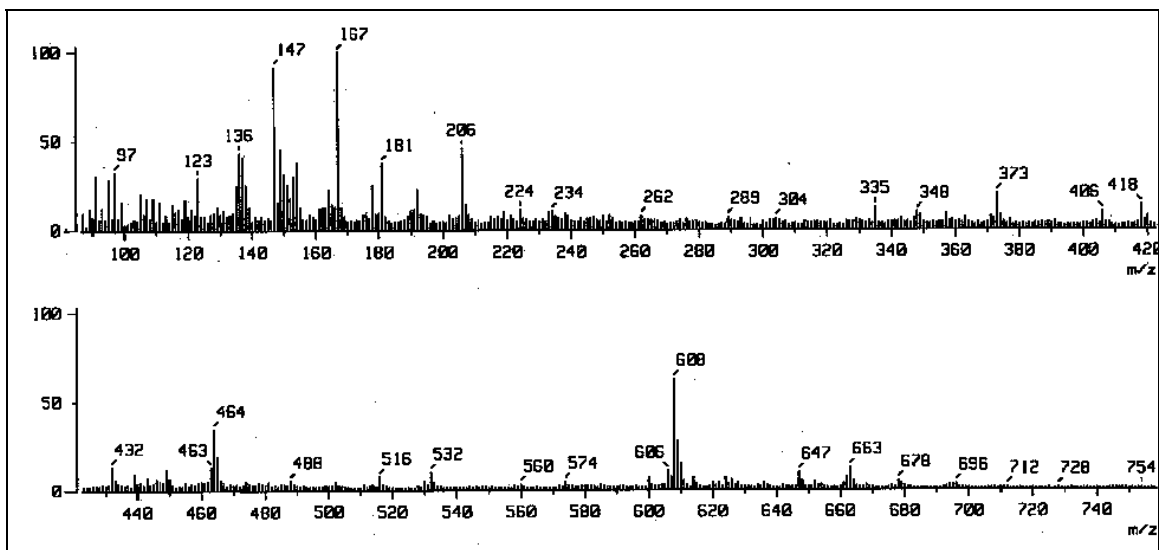


Fig. S22: FAB-MS spectrum of L<sub>1e</sub>.

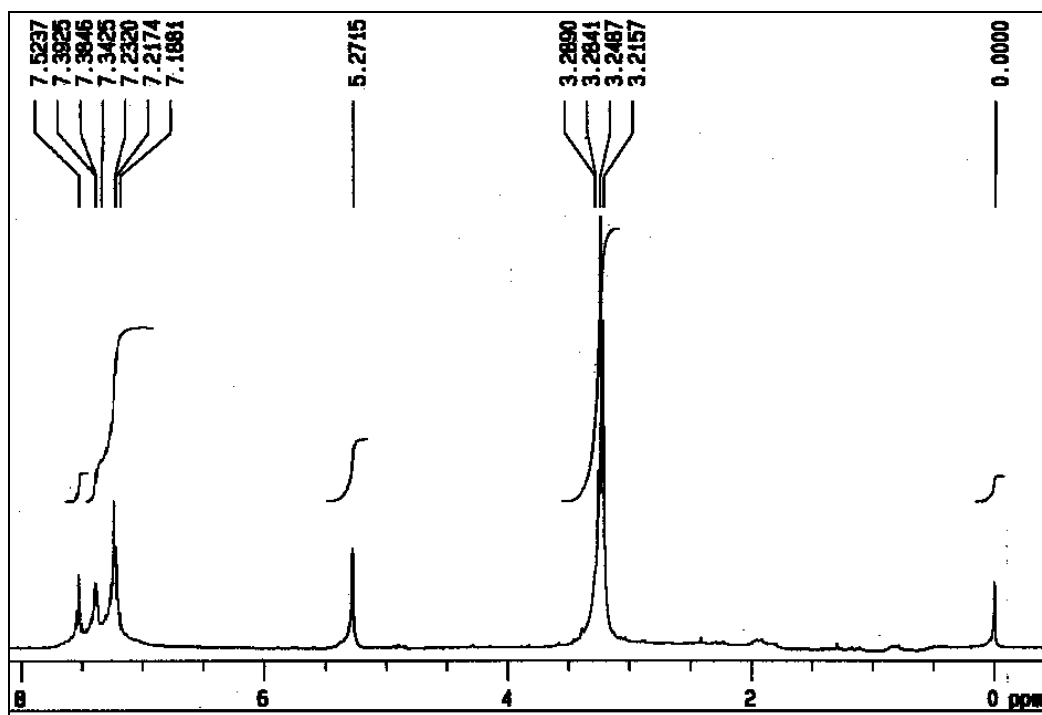


Fig. S23: 400 MHz <sup>1</sup>H-NMR spectrum of L<sub>2e</sub>.

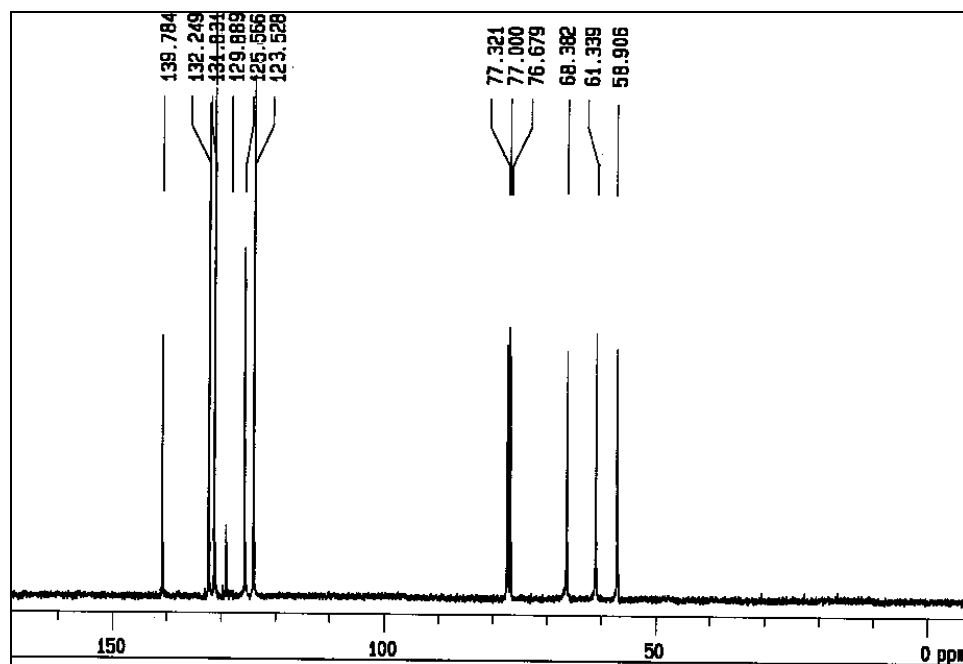


Fig. S24: 100 MHz  $^{13}\text{C}$ -NMR spectrum of  $\text{L}_{2e}$ .

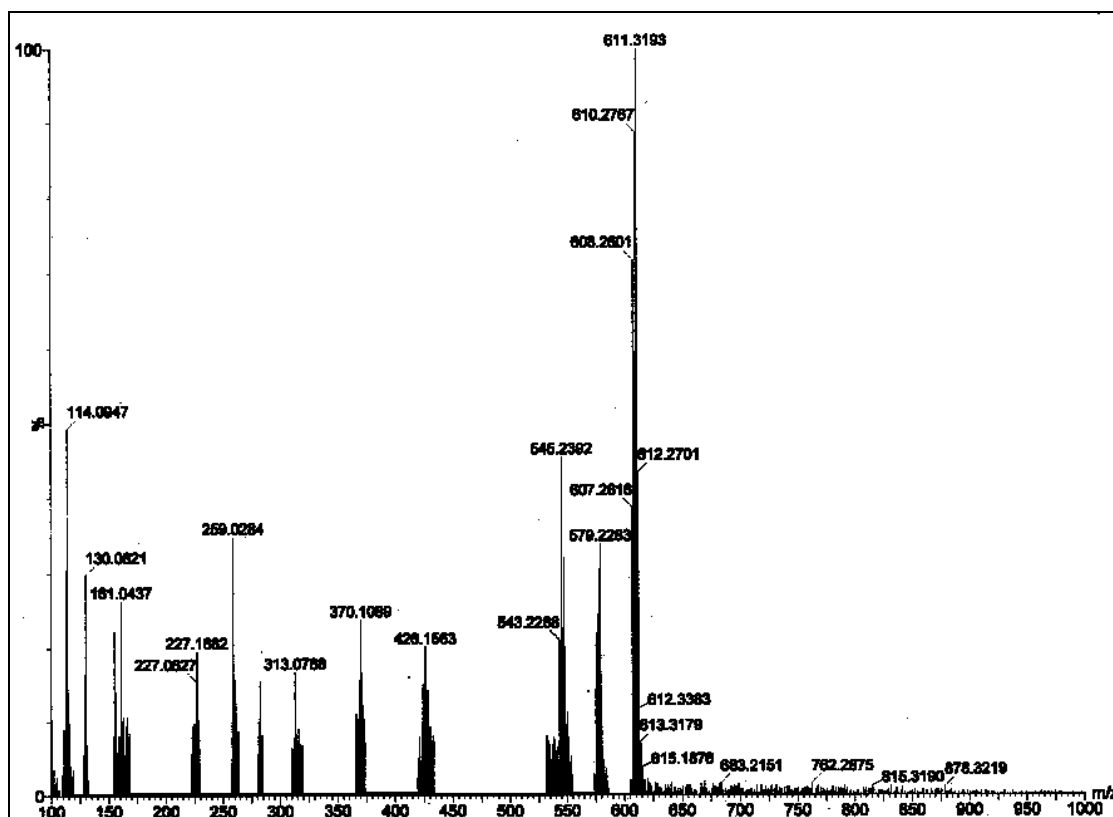


Fig. S25: ESI-MS spectrum of  $\text{L}_{2e}$ .

**Synthesis of tris-anthryl derivatives of the cryptands ( $L_1$ ,  $L_2$ ).** To a solution of  $L_{1e}$  (0.5 g, 0.8 mmol) in dry MeCN (20 mL), anhydrous  $K_2CO_3$  (2 g, excess) was added and stirred for 15 min. To this solution, 9-bromomethylantracene (0.67 g, 2.4 mmol) was added along with a crystal of KI and the reaction mixture was stirred first at RT for 1 h and then refluxed for 12 h when the solution became yellow in color. After cooling to RT, the solvent was removed under vacuum. The solid remained was washed several times with water, dissolved in  $CHCl_3$ , again washed several times with water and finally, the organic layer after drying over anhydrous  $Na_2SO_4$ , evaporated to dryness to obtain a yellow solid. The desired compound could be separated by silica gel column chromatography using chloroform: methanol in the ratio of 99:1 (v/v) as the eluent. Compound  $L_2$  was similarly synthesized taking  $L_{2e}$  in place of  $L_{1e}$ .

Compound  $L_1$  Yield: 57(%);  $^1H$  NMR (400 MHz,  $CDCl_3$ , 25 °C, TMS  $\delta$ ): 2.20-2.81 (m, 12H, 6  $\times$   $CH_2$ ), 3.37-3.55 (m, 12H, 6  $\times$   $CH_2$ ), 5.20 (s, 6H, 3  $\times$   $CH_2$ ), 5.35 (s, 6H, 3  $\times$  An- $CH_2$ ), 6.91 (d, 6H, An-H), 7.03 (d, 6H, An-H), 7.18 (m, 3H, Ar-H), 7.28 (m, 3H, Ar-H), 7.38 (m, 3H, Ar-H), 7.48 (m, 3H, Ar-H), 7.97 (d, 6H, An-H), 8.31 (d, 6H, An-H), 8.86 ppm (d, 3H, An-H);  $^{13}C\{^1H\}$  NMR (100 MHz,  $CDCl_3$ , 25 °C, TMS  $\delta$ ): 158.23, 141.13, 132.29, 131.34, 128.29, 125.58, 123.18, 114.12, 111.18, 108.19, 104.74, 68.05, 62.97, 58.04, 53.44 ppm; mp: 104 °C; FAB-MS (m/z): 1181(40) [ $L_1+2$ ] $^+$ . Anal. Calcd. for  $C_{78}H_{75}N_5S_3$ : C, 79.48; H, 6.41; N, 5.94 %. Found: C, 79.50; H, 6.48; N, 5.84 %.

Compound  $L_2$  Yield: 54(%);  $^1H$  NMR (400 MHz,  $CDCl_3$ , 25 °C, TMS  $\delta$ ): 2.60-2.72 (m, 12H, 6  $\times$   $CH_2$ ), 2.82-2.87 (m, 12H, 6  $\times$   $CH_2$ ), 5.36 (s, 6H, 3  $\times$   $CH_2$ ), 5.52 (s, 6H, 3  $\times$  An- $CH_2$ ), 7.14 (m, 3H, Ar-H), 7.25 (d, 6H, An-H), 7.39 (d, 6H, An-H), 7.47 (m, 3H, Ar-H), 7.73 (m, 3H, Ar-H), 7.87 (m, 3H, Ar-H), 7.99 (d, 6H, An-H), 8.32 (d, 6H, An-H), 8.39 ppm (d, 3H, An-H);  $^{13}C\{^1H\}$  NMR (100 MHz,  $CDCl_3$ , 25 °C, TMS  $\delta$ ): 157.13, 141.26, 133.24, 131.64, 128.32, 125.58, 124.13, 116.82, 113.79, 110.39, 106.23, 68.00, 61.99, 58.36, 53.84 ppm; FAB-MS (m/z): 1182 (50%) [ $L_2+3$ ] $^+$ . Anal. Calcd. for  $C_{78}H_{75}N_5S_3$ : C, 79.48; H, 6.41; N, 5.94 %. Found: C, 79.44; H, 6.38; N, 5.92 %.

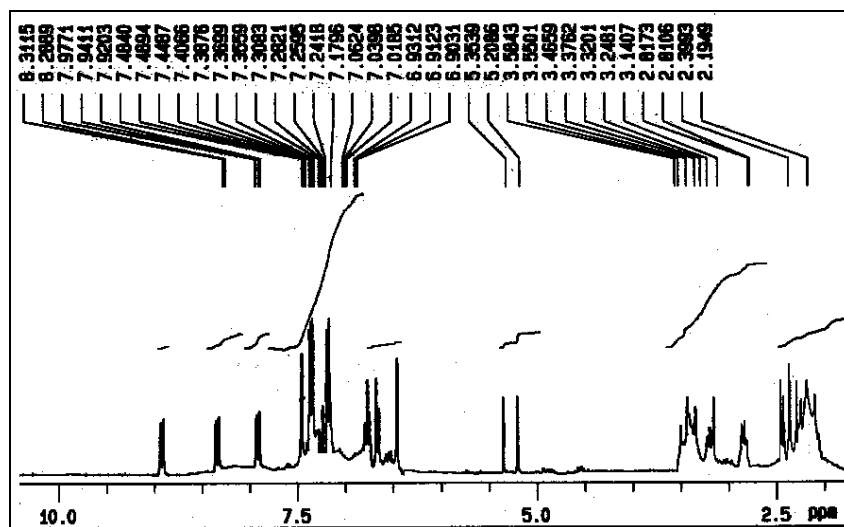


Fig. S26: 400 MHz  $^1H$ -NMR spectrum of  $L_1$ .

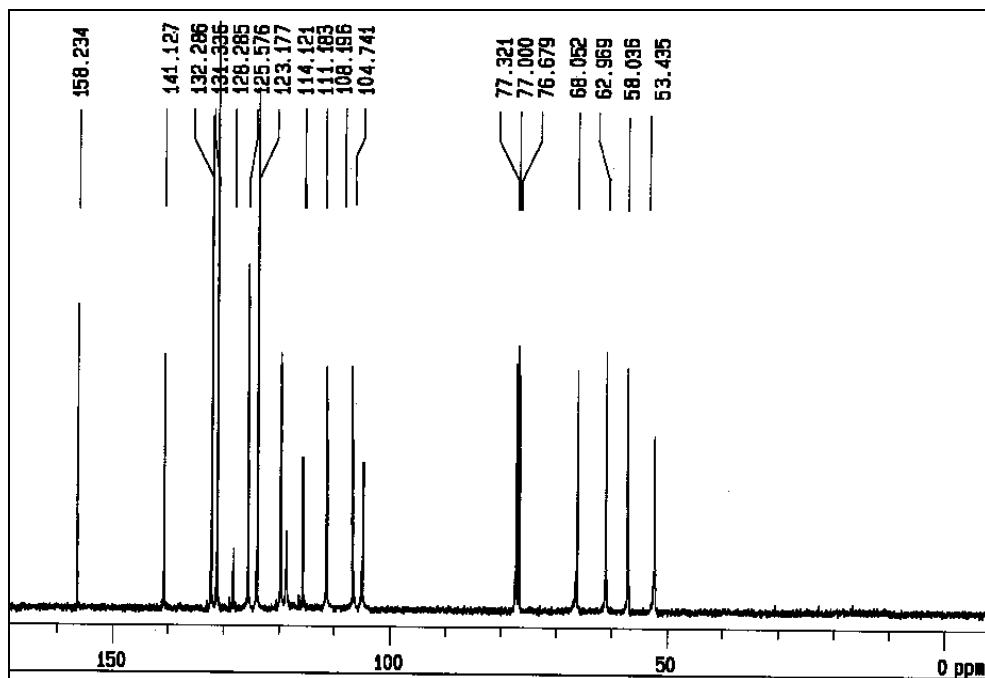


Fig. S27: 100 MHz  $^{13}\text{C}$ -NMR spectrum of  $\text{L}_1$ .

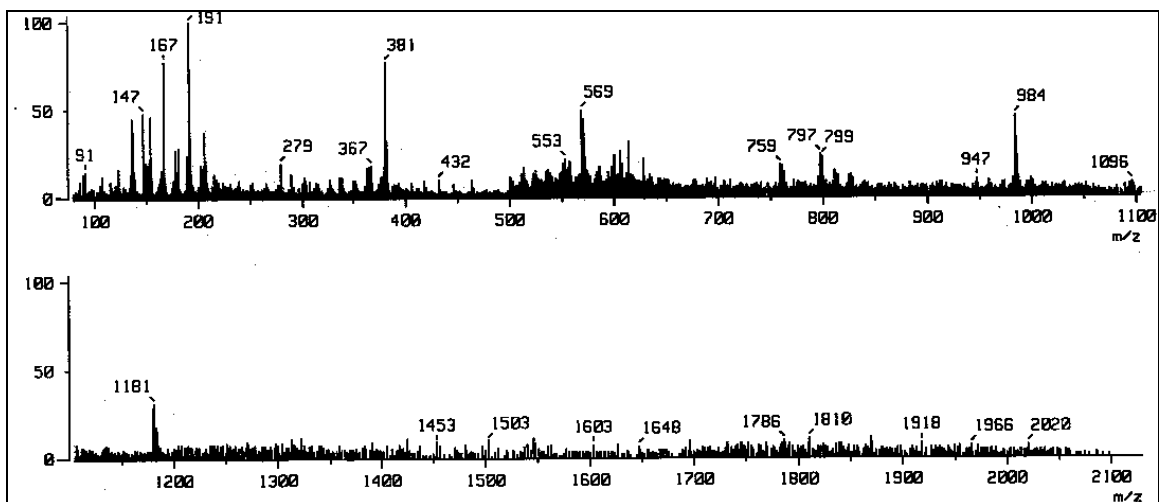


Fig. S28: FAB-MS spectrum of  $\text{L}_1$ .

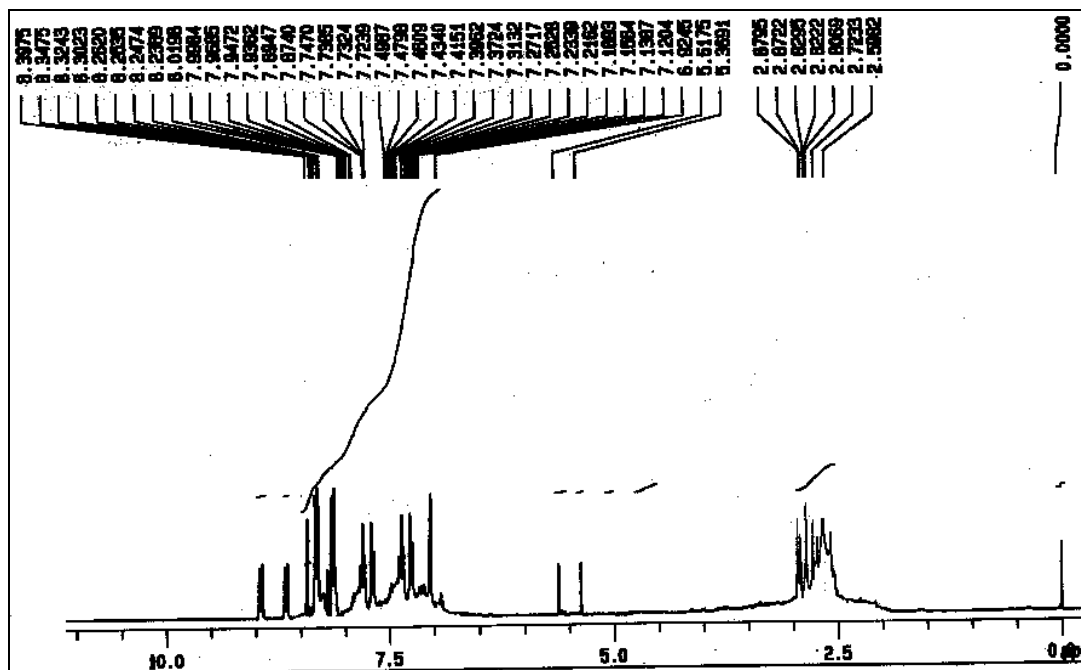


Fig. S29: 400 MHz  $^1\text{H}$ -NMR spectrum of  $\text{L}_2$ .

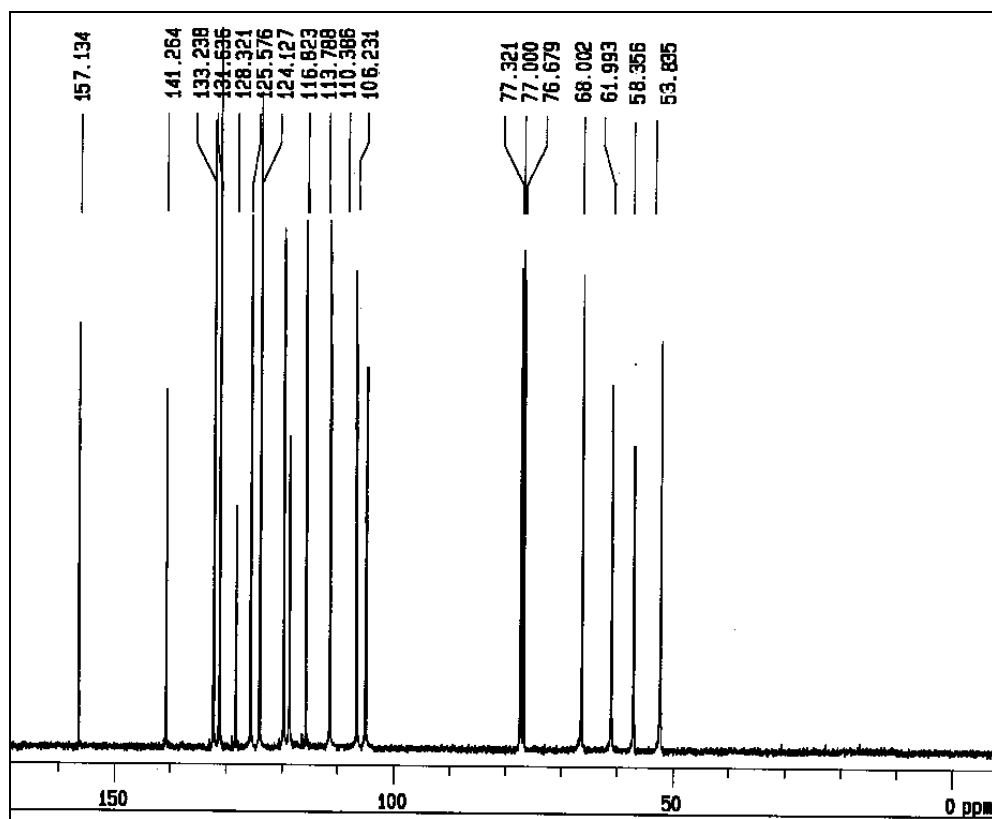


Fig. S30: 100 MHz  $^{13}\text{C}$ -NMR spectrum of  $\text{L}_2$ .

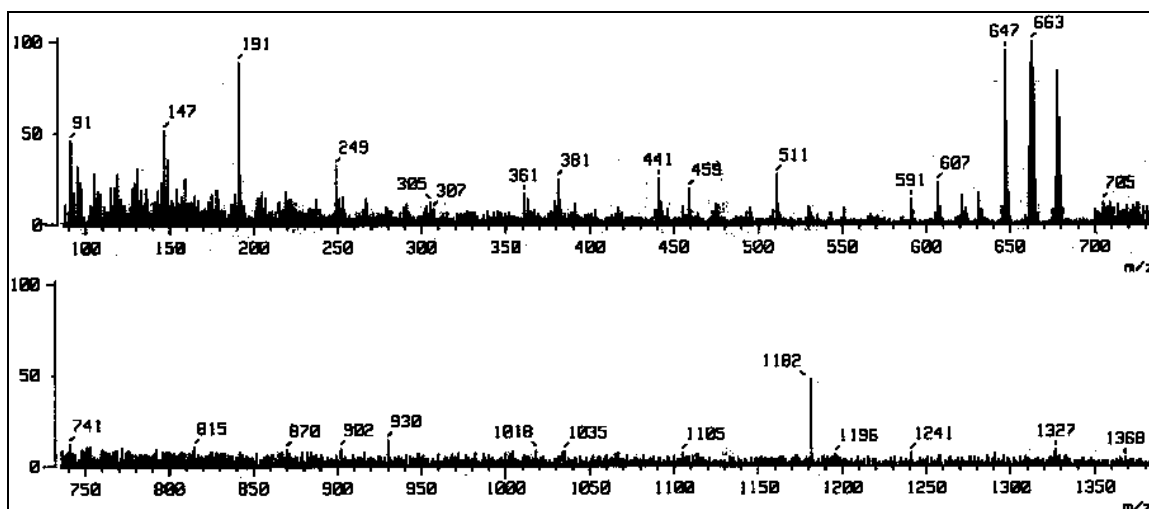


Fig. S31: FAB-MS spectrum of  $L_2$ .

**Synthesis of Cu(II) complexes of  $L_1$  and  $L_2$ .** To a stirring solution of  $L_1$  or  $L_2$  (0.1 mmol) in dry THF (20 ml), a THF solution (5 ml) of  $Cu(BF_4)_2 \cdot xH_2O$  (0.1 mmol) and stirred for 2 h at RT. After filtration, the filtrate was allowed to evaporate at RT whereupon a green solid separated. The solid was collected by filtration, washed with diethyl ether and dried under vacuum for use in emission measurements.

Compound  $L_1 \subset Cu(II)$  complex Yield: 79(%); ESI-MS (m/z): 621 (42%) [ $L_1 \subset Cu(II)$ ] $^{2+}$ .  
Anal. Calcd. for  $C_{78}H_{75}N_5S_3B_2F_8Cu$ : C, 66.17; H, 5.34; N, 4.95 %. Found: C, 66.04; H, 5.32; N, 4.99 %.

Compound  $L_2 \subset Cu(II)$  complex Yield: 64(%); ESI-MS (m/z): 621 (40%) [ $L_2 \subset Cu(II)$ ] $^{2+}$ .  
Anal. Calcd. for  $C_{78}H_{75}N_5S_3B_2F_8Cu$ : C, 66.17; H, 5.34; N, 4.95 %. Found: C, 66.24; H, 5.38; N, 4.90 %.

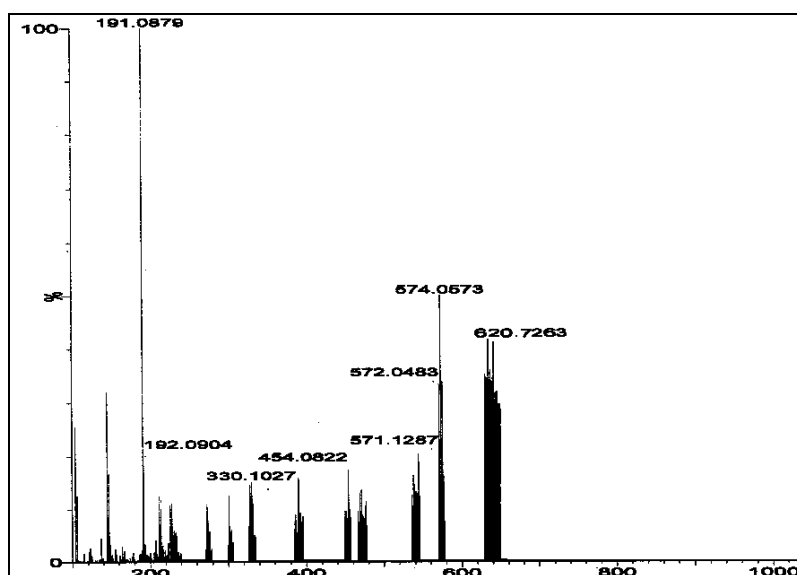


Fig. S32: ESI-MS spectrum of Cu(II) complex of  $L_1$ .

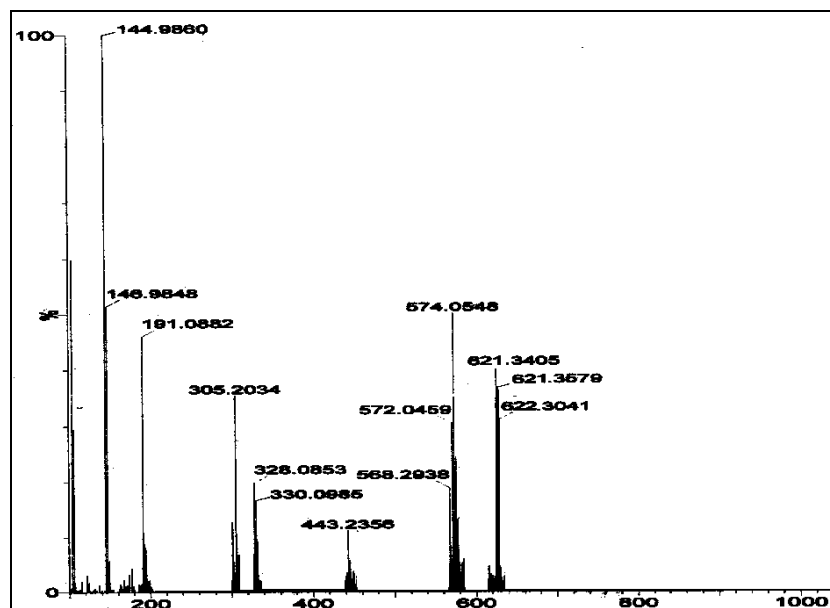


Fig. S33: ESI-MS spectrum of Cu(II) complexes of  $L_2$ .

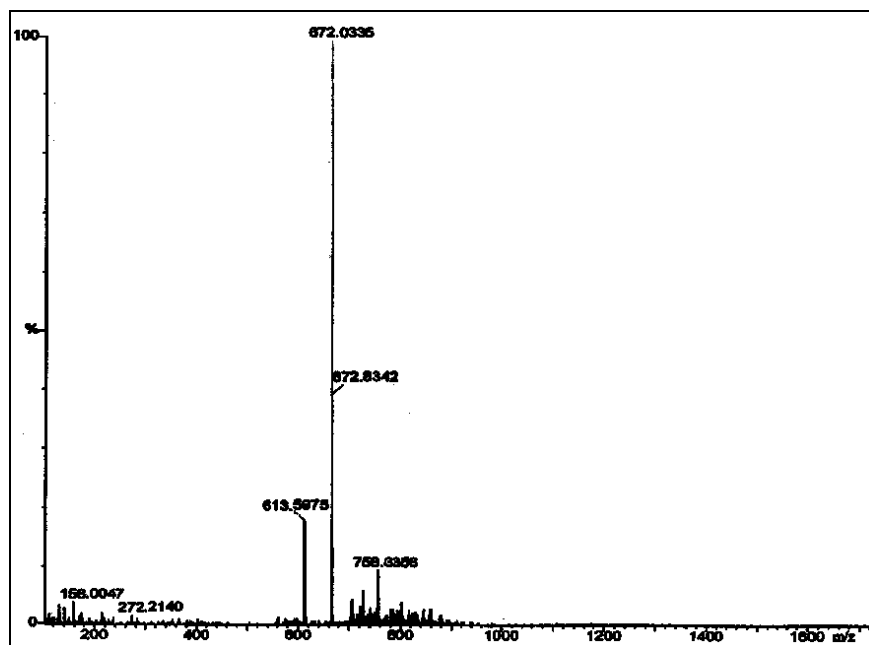


Fig. S34: ESI-MS spectrum after reduction of Cu(II)-cryptate of  $L_{2e}$ .

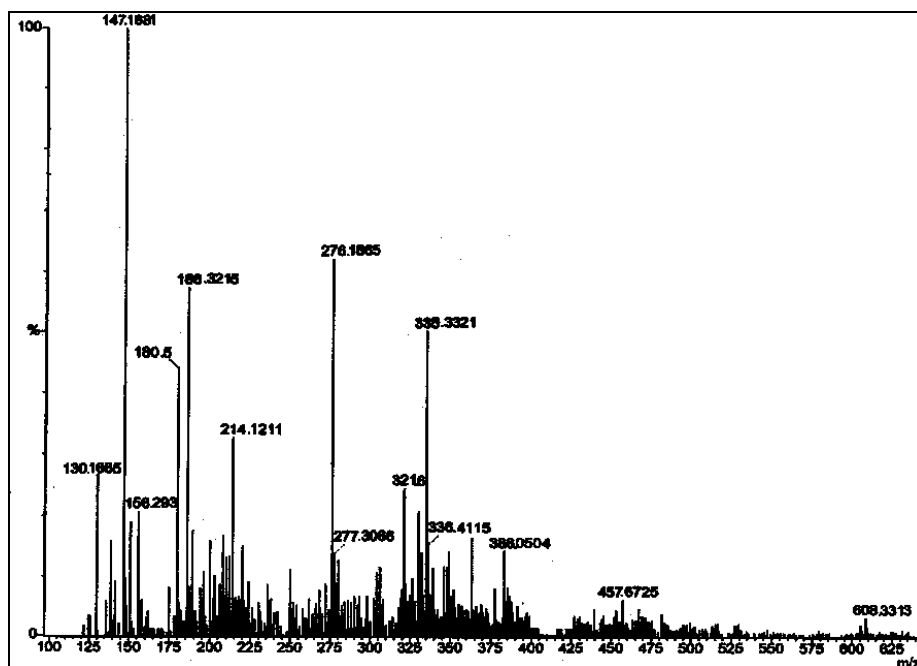


Fig. S35: ESI-MS spectrum of Cu(II)-cryptate of L<sub>2e</sub>.

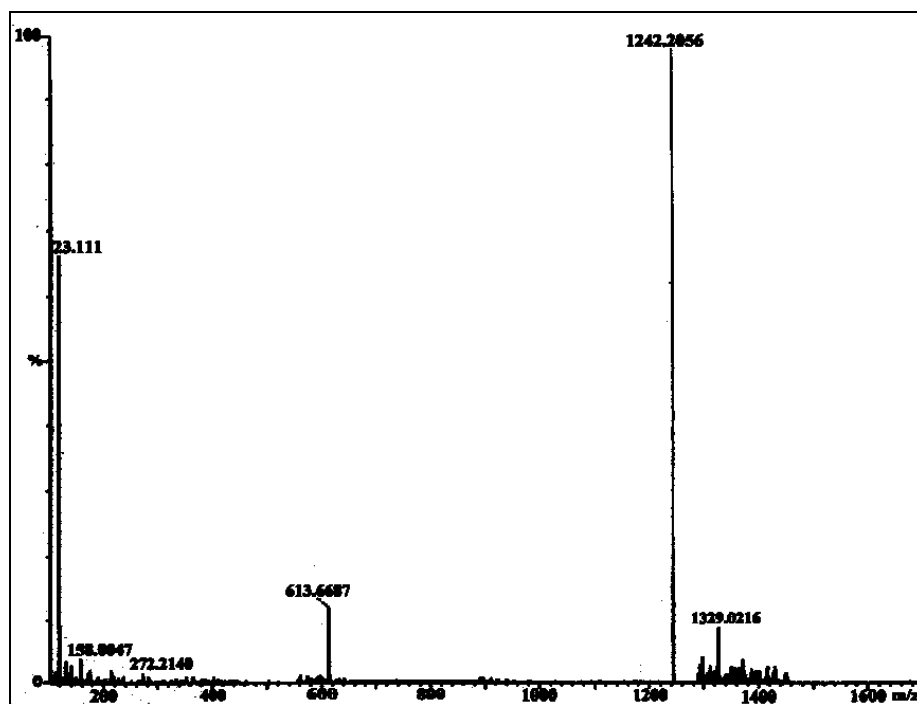


Fig. S36: ESI-MS spectrum after reduction of Cu(II)-cryptate of L<sub>2</sub>.

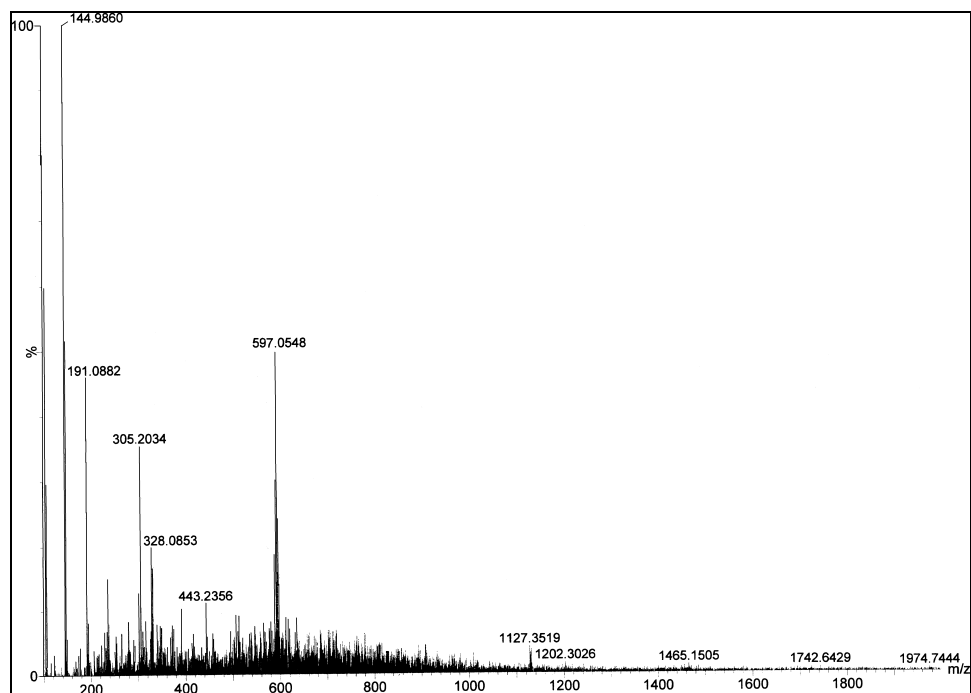


Fig. S37: ESI-MS spectrum of Cu(II)-cryptate of L<sub>3</sub>.

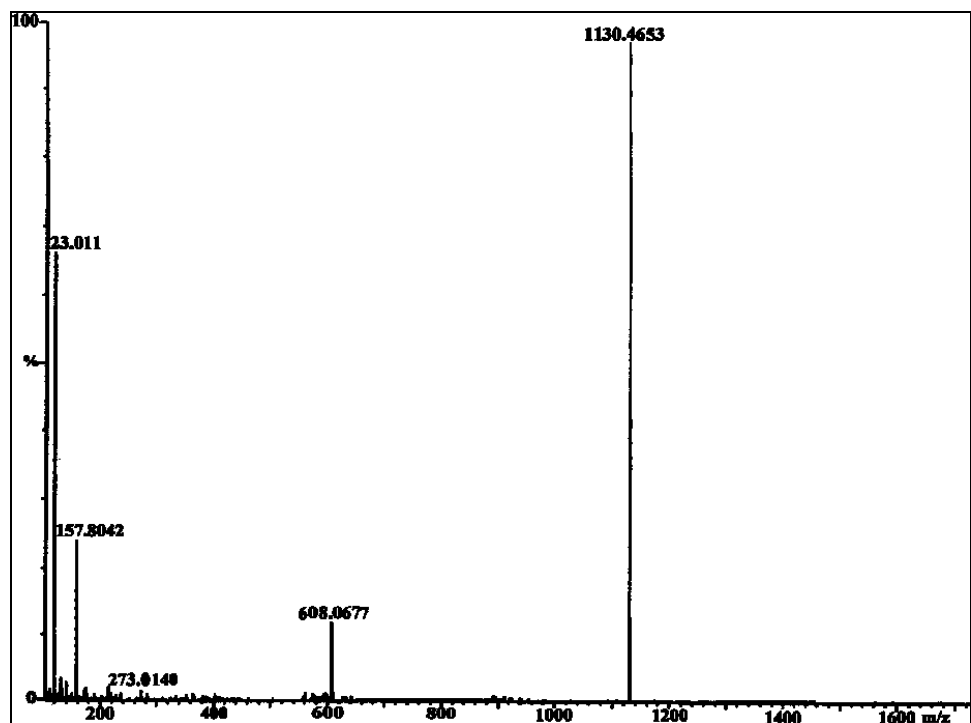
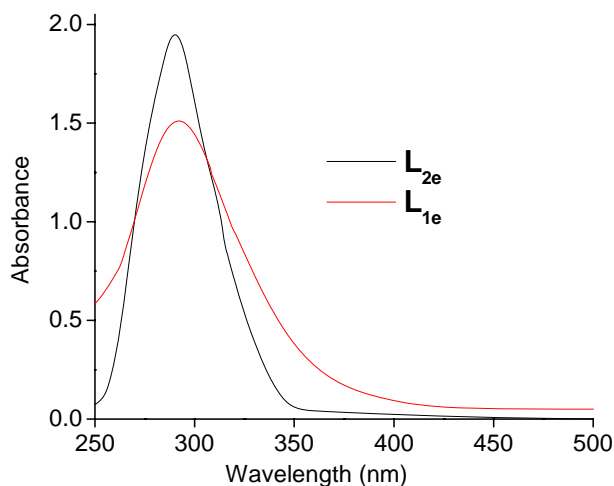
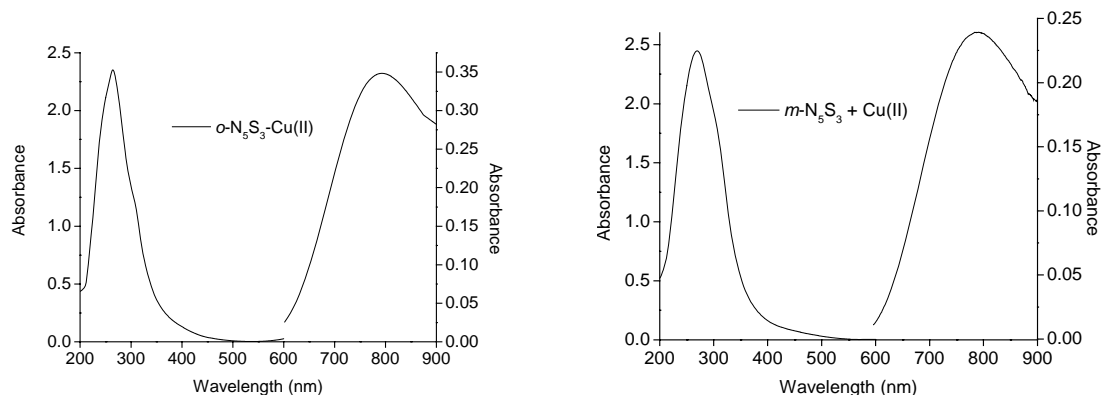


Fig. S38: ESI-MS spectrum after reduction of Cu(II)-cryptate of L<sub>3</sub>.



**Fig. S39:** Absorption spectra of  $L_{1e}$  and  $L_{2e}$  THF (Conc. of  $L_{1e}$  =  $1.2 \times 10^{-4}$  M and Conc. of  $L_{2e}$  =  $1.4 \times 10^{-4}$  M).



**Fig. S40:** Absorption spectra of  $L_{1e}+Cu(II)$  and  $L_{2e}+Cu(II)$  in THF.

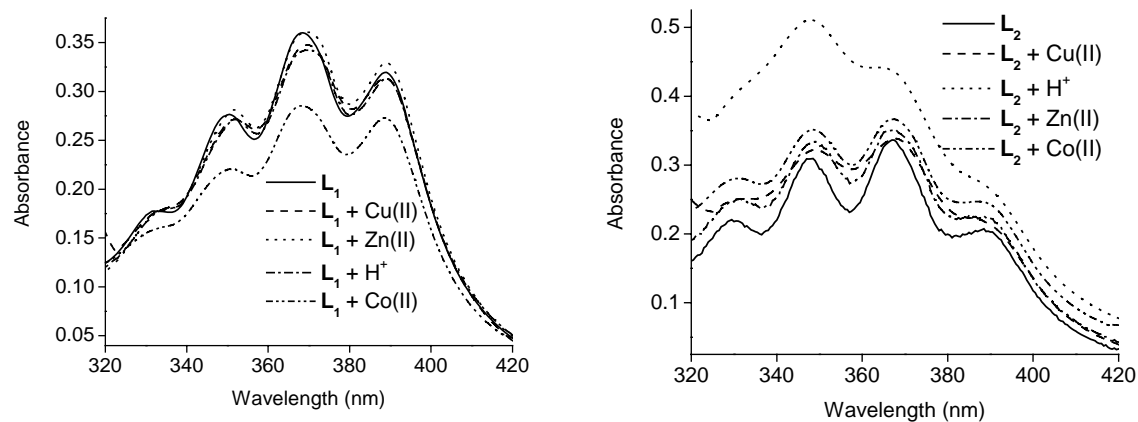


**Fig. S41.** (a) UV-vis spectra of  $L_1$ ,  $L_1+Cu(II)$ ,  $L_1+Zn(II)$ ,  $L_1+H^+$ ,  $L_1+Co(II)$  (conc. of  $L_1$  =  $1.32 \times 10^{-5}$  M) in THF, (b) UV-vis spectra of  $L_2$ ,  $L_2+Cu(II)$ ,  $L_2+Zn(II)$ ,  $L_2+H^+$ ,  $L_2+Co(II)$  (conc. of  $L_2$  =  $1.3 \times 10^{-5}$  M) in THF.

**TABLE S1:** Absorption and molar extinction coefficient ( $\epsilon$ ) of **L<sub>1</sub>** alone and in presence of different metal ions in THF (Conc. of **L<sub>1</sub>** =  $1.32 \times 10^{-5}$  M).

	Absorption $\lambda$ , nm ( $\epsilon$ , $\text{dm}^3 \text{mol}^{-1} \text{cm}^{-1}$ )				
<b>L<sub>1</sub></b>	389 (24302)	369 (27336)	350 (21009)	331 (13521)	258 (188583)
<b>L<sub>1</sub>+Mn(II)</b>	390 (25502)	370 (28084)	352 (21845)	333 (13893)	259 (187417)
<b>L<sub>1</sub>+Co(II)</b>	389 (21012)	369 (21781)	350 (16915)	333 (12195)	295 (161008)
<b>L<sub>1</sub>+Ni(II)</b>	389 (24092)	370 (26480)	352 (20417)	335 (12927)	258 (180598)
<b>L<sub>1</sub>+Cu(II)</b>	389 (24184)	370 (26506)	352 (20962)	333 (13558)	262 (220109)
<b>L<sub>1</sub>+Zn(II)</b>	389 (25064)	370 (27474)	352 (21380)	332 (13436)	258 (184551)
<b>L<sub>1</sub>+Cd(II)</b>	389 (24595)	370 (26945)	352 (20973)	334 (13277)	258 (182004)
<b>L<sub>1</sub>+Ag(I)</b>	389 (24527)	370 (26726)	352 (21130)	333 (13523)	259 (181199)
<b>L<sub>1</sub>+Tl(I)</b>	389 (24221)	370 (26923)	352 (20995)	333 (13617)	259 (182230)
<b>L<sub>1</sub>+H<sup>+</sup></b>	389 (23830)	370 (26022)	352 (20723)	335 (13727)	258 (179478)

**TABLE S2:** Absorption and molar extinction coefficient ( $\epsilon$ ) of **L<sub>2</sub>** alone and in presence of different metal ions in THF (Conc. of **L<sub>2</sub>** =  $1.3 \times 10^{-5}$  M).

	Absorption $\lambda$ , nm ( $\epsilon$ , $\text{dm}^3 \text{mol}^{-1} \text{cm}^{-1}$ )				
<b>L<sub>2</sub></b>	389 (15963)	367 (25884)	349 (23808)	330 (16998)	260 (163747)
<b>L<sub>2</sub>+Mn(II)</b>	389 (18648)	368 (28188)	348 (26861)	331 (21125)	261 (170766)
<b>L<sub>2</sub>+Co(II)</b>	389 (19243)	367 (28545)	349 (27310)	330 (21791)	261 (171204)
<b>L<sub>2</sub>+Ni(II)</b>	389 (14066)	366 (27899)	348 (25828)	330 (18505)	261 (165958)
<b>L<sub>2</sub>+Cu(II)</b>	391 (24184)	366 (24321)	349 (23264)	330 (16793)	266 (206814)
<b>L<sub>2</sub>+Zn(II)</b>	389 (17176)	366 (27039)	349 (25710)	330 (19009)	261 (166876)
<b>L<sub>2</sub>+Cd(II)</b>	389 (15650)	366 (25324)	347 (25488)	330 (20336)	260 (160454)
<b>L<sub>2</sub>+Ag(I)</b>	390 (15981)	366 (23865)	349 (22455)	330 (17298)	260 (158809)
<b>L<sub>2</sub>+Tl(I)</b>	389 (16337)	368 (26101)	348 (24335)	330 (17453)	261 (164948)
<b>L<sub>2</sub>+H<sup>+</sup></b>	389 (10111)	366 (16182)	347 (16728)	331 (13988)	258 (141818)

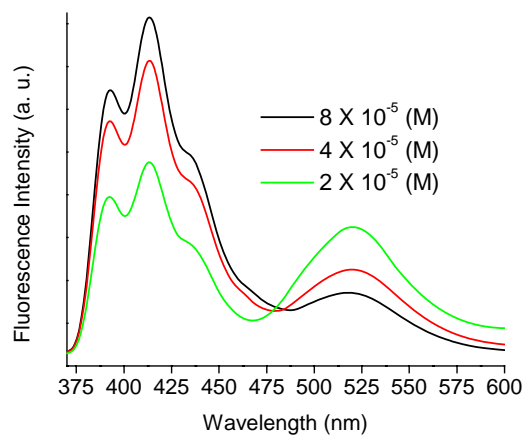


**Fig. S42.** Fluorescence emission of  $L_1$  in dry THF at different concentrations.

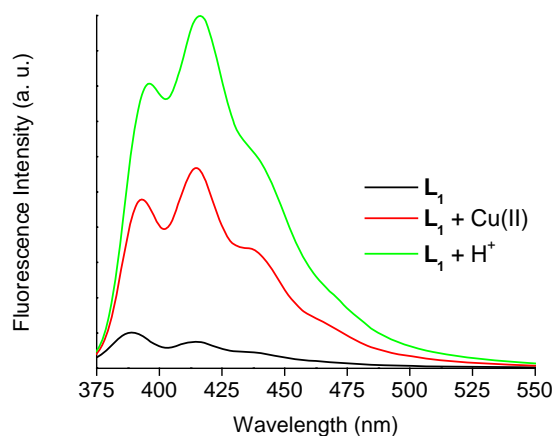


**Fig. S43:** Emission spectra of  $L_1$  in presence of different ionic inputs in THF:H<sub>2</sub>O, 90:10. Plot for controlled experiments.

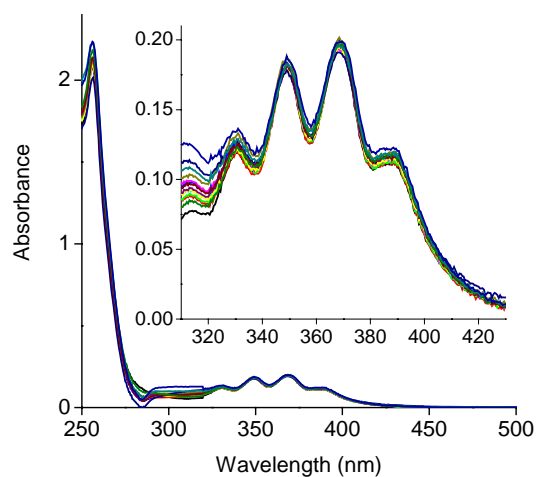


**Fig. S44:** Absorption spectra of  $L_1$  in presence of Cu(II) ionic input in THF.

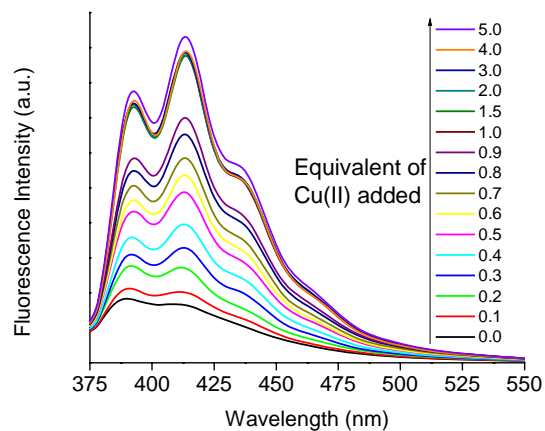


**Fig. S45:** Emission spectra of  $L_1$  in presence of  $Cu(II)$  ionic input in THF.

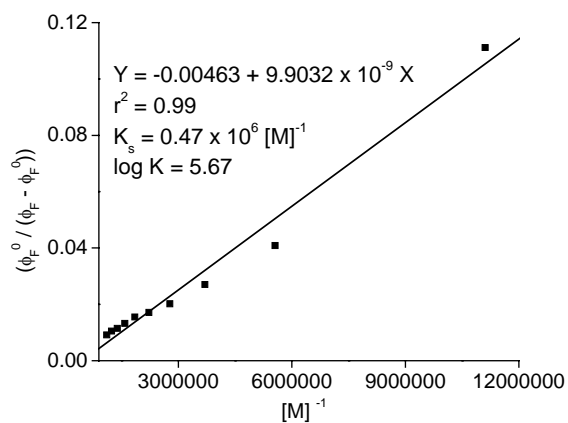


**Fig. S46:** Linear regression plot for complex stability constant determination of  $L_1$  in presence of  $Cu(II)$  in THF.

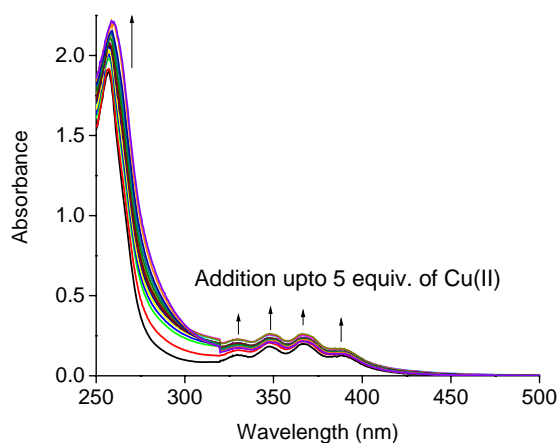


**Fig. S47:** Absorption spectra of  $L_2$  in presence of  $Cu(II)$  ionic input in THF.

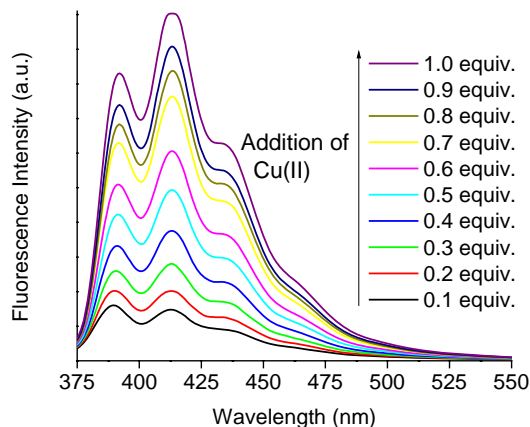


**Fig. S48:** Emission spectra of  $L_2$  in presence of  $Cu(II)$  ionic input in THF.

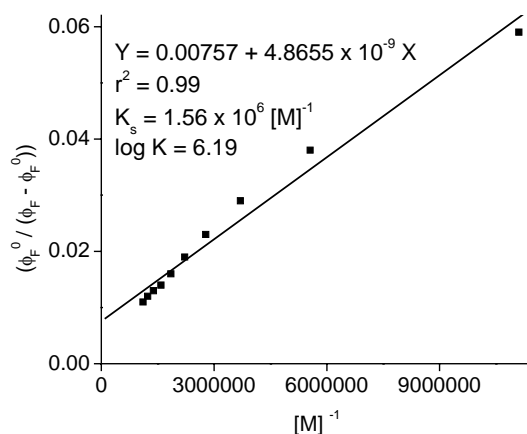


**Fig. S49:** Linear regression plot for complex stability constant determination of  $L_2$  in presence of  $Cu(II)$  in THF.

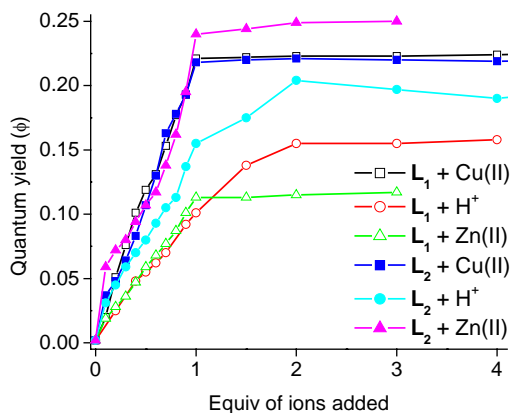


**Fig. S50.** Plot of the quantum yields of  $L_1$  and  $L_2$  (concentration of  $L_1$  and  $L_2 = 1.0 \times 10^{-7} M$ ) as a function of equivalents of  $Cu(II)$ ,  $Zn(II)$  ions and protons in THF.

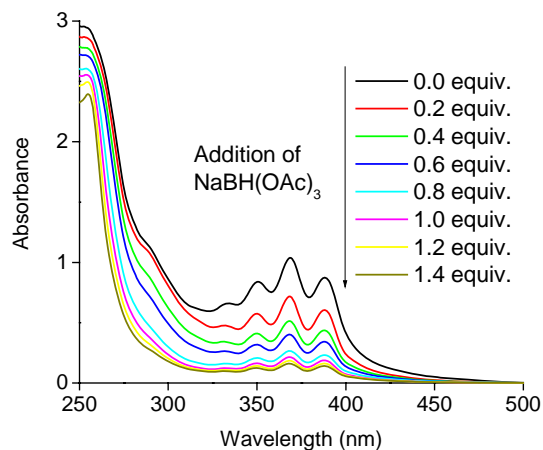


**Fig. S51:** Absorption spectra of  $L_1-Cu(II)$  in presence of  $NaBH(OAc)_3$  solution in THF as input.

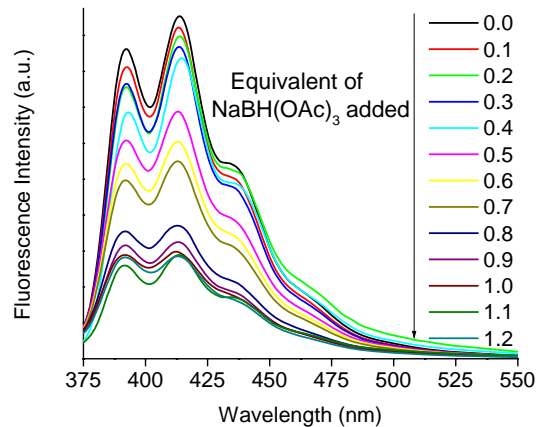


**Fig. S52:** Emission spectra of  $L_1-Cu(II)$  in presence of  $NaBH(OAc)_3$  solution in THF as input.

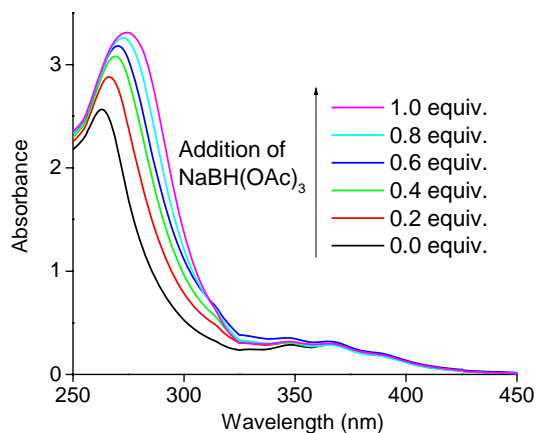


**Fig. S53:** Absorption spectra of  $L_2-Cu(II)$  in presence of  $NaBH(OAc)_3$  solution in THF as input.

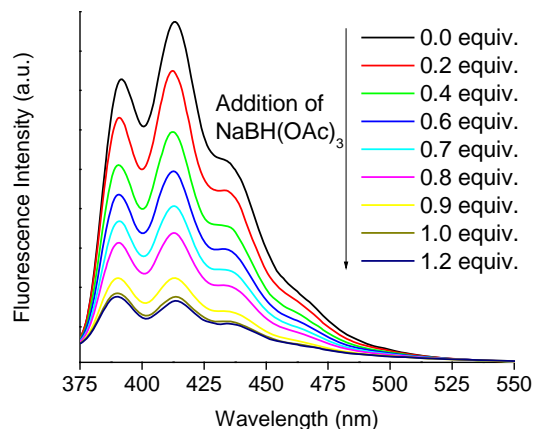


**Fig. S54:** Emission spectra of  $L_2\text{-Cu(II)}$  in presence of  $\text{NaBH(OAc)}_3$  solution in THF as input.

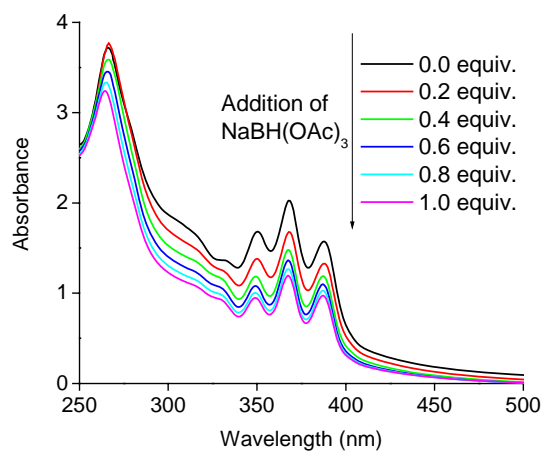


**Fig. S55:** Absorption spectra of  $L_3\text{-Cu(II)}$  in presence of  $\text{NaBH(OAc)}_3$  solution in THF as input.

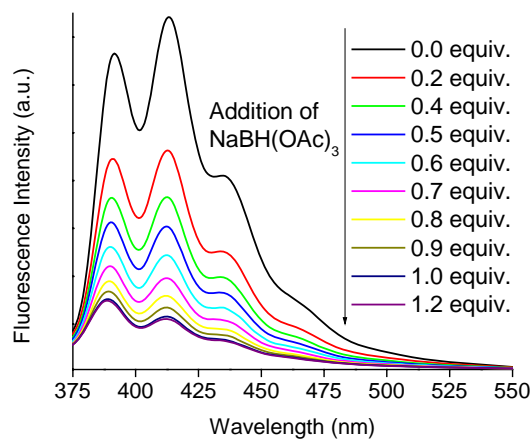


**Fig. S56:** Emission spectra of  $L_3\text{-Cu(II)}$  in presence of  $\text{NaBH(OAc)}_3$  solution in THF as input.

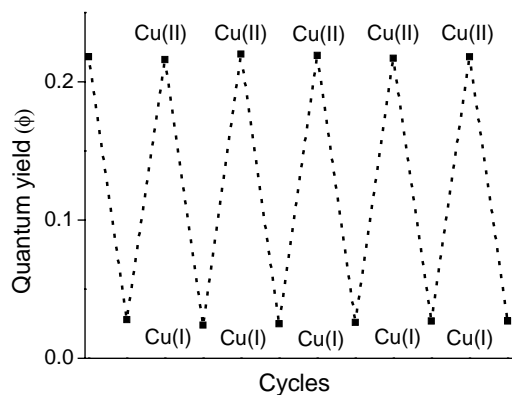


**Fig. S57:** Quantum yield plot of  $L_2Cu(II)$  complex after the reduction by  $NaBH(OAc)_3$  and the corresponding aerial oxidation after 12hrs. Molecular switch 'ON-OFF' representation.

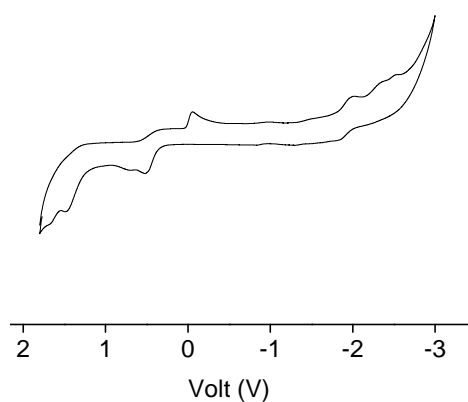


**Fig. S58:** Cyclic voltammogram of  $L_1Cu(II)$  in THF solution recorded at a glassy carbon as working electrode, with Ag/AgCl reference electrode

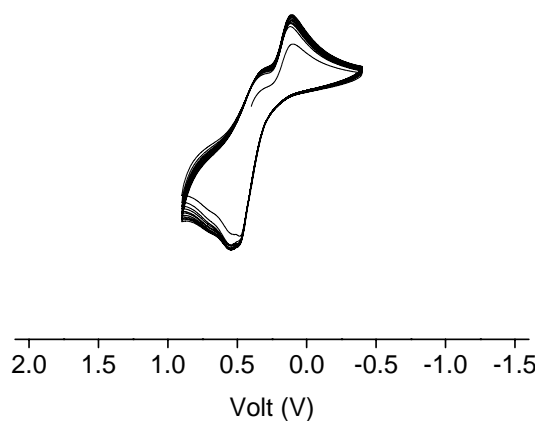


**Fig. S59:** Continuous cyclic voltammogram of  $L_1Cu(II)$  (selected part) in THF solution recorded at a glassy carbon as working electrode, with Ag/AgCl reference electrode

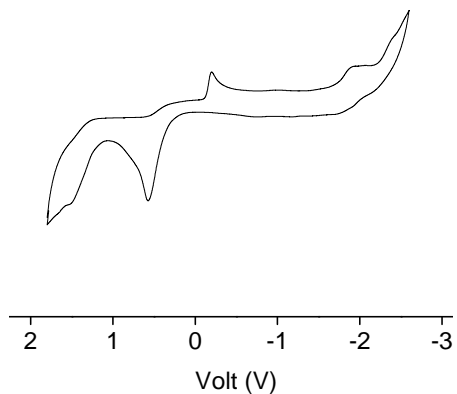


**Fig. S60:** Cyclic voltammogram of  $L_2Cu(II)$  in THF solution recorded at a glassy carbon as working electrode, with Ag/AgCl reference electrode

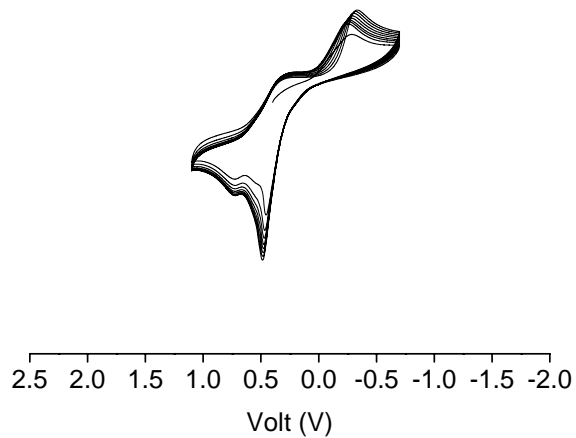


**Fig. S61:** Continuous cyclic voltammogram of  $L_2Cu(II)$  (selected part) in THF solution recorded at a glassy carbon as working electrode, with Ag/AgCl reference electrode